Title

Requirement of GrgA for Chlamydia infectious progeny production, optimal growth, and efficient plasmid maintenance.

Journal

mBio, 15(1)

Authors

Lu, Bin

Wang, Yuxuan

Wurihan, Wurihan

et al.

Publication Date

2024-01-16

DOI

10.1128/mbio.02036-23

Peer reviewed

AMERICAN SOCIETY FOR MICROBIOLOGY | mBio

Check for updates

| Bacteriology | Research Article

Requirement of GrgA for *Chlamydia* infectious progeny production, optimal growth, and efficient plasmid maintenance

Bin Lu,[1,2] Yuxuan Wang,[2] Wurihan Wurihan,[2] Andrew Cheng,[2] Sydney Yeung,[2] Joseph D. Fondell,[2] Zhao Lai,[3,4] Danny Wan,[2] Xiang Wu,[1] Wei Vivian Li,[5] Huizhou Fan[2]

AUTHOR AFFILIATIONS See affiliation list on p. 23.

ABSTRACT *Chlamydia*, an obligate intracellular bacterial pathogen, has a unique developmental cycle involving the differentiation of invading elementary bodies (EBs) to noninfectious reticulate bodies (RBs), replication of RBs, and redifferentiation of RBs into progeny EBs. Progression of this cycle is regulated by three sigma factors, which direct the RNA polymerase to their respective target gene promoters. We hypothesized that the *Chlamydia*-specific transcriptional regulator GrgA, previously shown to activate σ66 and σ28, plays an essential role in chlamydial development and growth. To test this hypothesis, we applied a novel genetic tool known as dependence on plasmid-mediated expression to create *Chlamydia trachomatis* with conditional GrgA deficiency. We show that GrgA-deficient *C. trachomatis* RBs have a growth rate that is approximately half of the normal rate and fail to transition into progeny EBs. In addition, GrgA-deficient *C. trachomatis* fails to maintain its virulence plasmid. Results of RNA-Seq analysis indicate that GrgA promotes RB growth by optimizing tRNA synthesis and expression of nutrient-acquisition genes, while it enables RB-to-EB conversion by facilitating the expression of a histone and outer membrane proteins required for EB morphogenesis. GrgA also regulates numerous other late genes required for host cell exit and subsequent EB invasion into host cells. Importantly, GrgA stimulates the expression of σ54, the third and last sigma factor, and its activator, AtoC, and thereby indirectly upregulating the expression of σ54-dependent genes. In conclusion, our work demonstrates that GrgA is a master transcriptional regulator in *Chlamydia* and plays multiple essential roles in chlamydial pathogenicity.

IMPORTANCE Hallmarks of the developmental cycle of the obligate intracellular pathogenic bacterium *Chlamydia* are the primary differentiation of the infectious elementary body (EB) into the proliferative reticulate body (RB) and the secondary differentiation of RBs back into EBs. The mechanisms regulating these transitions remain unclear. In this report, we developed an effective novel strategy termed dependence on plasmid-mediated expression (DOPE) that allows for the knockdown of essential genes in *Chlamydia*. We demonstrate that GrgA, a *Chlamydia*-specific transcription factor, is essential for the secondary differentiation and optimal growth of RBs. We also show that GrgA, a chromosome-encoded regulatory protein, controls the maintenance of the chlamydial virulence plasmid. Transcriptomic analysis further indicates that GrgA functions as a critical regulator of all three sigma factors that recognize different promoter sets at developmental stages. The DOPE strategy outlined here should provide a valuable tool for future studies examining chlamydial growth, development, and pathogenicity.

KEYWORDS *Chlamydia*, GrgA, transcriptional regulation, transcription factors, regulation of gene expression

Editor Paul Babitzke, The Pennsylvania State University, University Park, Pennsylvania, USA

Address correspondence to Xiang Wu, wxspring@126.com, or Huizhou Fan, fanhu@rwjms.rutgers.edu.

Bin Lu and Yuxuan Wang contributed equally to this article. Author order was determined in order of increasing seniority in the project.

The authors declare no conflict of interest.

See the funding table on p. 24.

Received 1 August 2023
Accepted 16 November 2023
Published 19 December 2023

Chlamydia is an obligate intracellular bacterium possessing a unique developmental cycle (1). The cycle involves two morphologically and functionally distinct cell types known as the elementary body (EB) and reticulate body (RB). The EB, approximately 0.3 µm in diameter, has DNA condensed by histones (2, 3) and an outer membrane containing proteins crosslinked with disulfides (4). It is capable of temporary survival in extracellular environments despite having limited metabolic activities and is responsible for infecting host cells to initiate the developmental cycle. After EB is inside a host cell, its cysteine-rich outer membrane proteins undergo reduction, and DNA decondensation occurs. These processes enable EBs to differentiate into larger (approximately 1 µm in diameter) RBs that replicate within a cytoplasmic vacuole known as an inclusion. After multiple rounds of replication, RBs asynchronously differentiate back into non-replicating EBs (1, 5). The newly formed EBs, upon release from host cells, can either infect other cells within the same host or transfer to new hosts. Unlike EBs, any released RBs are unable to initiate new developmental cycles.

The chlamydial developmental cycle is transcriptionally regulated (1, 6, 7). After EBs enter host cells, early genes are activated during the first few hours enabling primary differentiation into RBs. Starting at around 8 h post-infection, midcycle genes, representing the vast majority of all chlamydial genes, are expressed enabling RB replication. At around 24 h post-infection, late genes are activated to enable the secondary differentiation of RBs back into EBs.

Sigma factor is a subunit of the RNA polymerase (RNAP) holoenzyme that recognizes and binds specific DNA gene promoter elements, allowing RNAP to initiate transcription (8). *Chlamydia* encodes three different sigma factors termed σ66, σ28, and σ54 (9, 10). σ66 RNAP holoenzyme is active throughout the developmental cycle, whereas the σ28 and σ54 RNAP holoenzymes transcribe only a subset of late or mid-late genes (11–13).

GrgA is a *Chlamydia*-specific transcriptional regulator that binds both to σ66 and σ28 and activates the transcription of numerous chlamydial genes *in vitro* and *in vivo* (14–16). RNA-Seq analysis of *Chlamydia trachomatis* conditionally overexpressing GrgA, along with GrgA *in vitro* transcription assays, revealed two other transcription factor-encoding genes, *euo* and *hrcA*, as members of the GrgA regulon (14). Both *euo* and *hrcA* are transcribed during the early phase and midcycle (14). Euo acts as a repressor of chlamydial late genes (17), while HrcA regulates the expression of multiple protein chaperones (18), crucial for bacterial growth (19). These findings suggest GrgA plays an important regulatory role in chlamydial development.

Despite recent advancements in the genetic manipulation of *Chlamydia* (20, 21), the tools available to study essential genes in this obligate intracellular bacterium remain limited. We attempted but failed to disrupt *grgA* through group II intron (Targetron) insertional mutagenesis (22). Previously, the Valdivia group was also unable to generate *grgA*-null mutants using chemical mutagenesis (23). Given that Targetron and chemical mutagenesis have been successfully used to disrupt numerous non-essential chlamydial genes [e.g., (24–30)], these negative results suggest that *grgA* is an essential gene for *Chlamydia* viability. In this work, we confirm that *grgA* is indeed an essential gene by using a novel genetic tool that we term DOPE (dependence on plasmid-mediated expression). Importantly, we show that GrgA is necessary for RB-to-EB differentiation and is also required for optimal RB growth. We further demonstrate that GrgA regulates the maintenance of the normal copy number of the plasmid, which encodes Pgp3 (a secreted virulence factor), Pgp4 (a transcriptional regulator of specific chromosomal genes as well as Pgp3), and proteins involved in plasmid replication (31–33). These findings provide further evidence that GrgA is a major regulator of σ66, σ28, and σ54 target genes, and plays important regulatory roles in governing the chlamydial developmental cycle.

RESULTS

DOPE enables *grgA* disruption

Targetron is a group II intron-based insertional mutagenesis technology that has been used successfully to disrupt numerous chlamydial chromosomal genes (24–30). In an effort to knock out GrgA expression in *Chlamydia* and investigate its physiological functions, we utilized Targetron vectors containing spectinomycin-resistance gene-bearing group II introns specific for multiple *grgA* insertion sites. Whereas we did obtain spectinomycin-resistant chlamydiae, diagnostic PCR analysis detected the intron but not within *grgA*. Taken together with the earlier unsuccessful attempts to generate *grgA*-null mutants using chemical mutagenesis (23), we hypothesized that *grgA* is an essential gene and, as such, not amenable to conventional mutagenesis approaches.

To circumvent this issue, we devised a strategy we term DOPE to investigate the biological functions of essential genes in *Chlamydia*. Although disruption of essential genes in the wild-type bacterium causes lethality, transforming *Chlamydia* with a recombinant plasmid carrying the essential chromosomal gene downstream of an inducible promoter allows for the disruption of the chromosomal allele when the inducer is present in the culture medium. This method generates a strain with a disrupted essential gene, where withdrawal of the inducer will cause depletion of the gene products from the recombinant plasmid, allowing functional and mechanistic analyses of the essential gene.

We applied DOPE to study GrgA by constructing a shuttle vector named pGrgA-DOPE, which encodes an anhydrotetracycline (ATC)-inducible *grgA* allele (plasmid-encoded inducible *grgA* or peig) (Fig. S1). In addition to the replication origin, we kept all eight genes encoded by the wild-type *C. trachomatis* plasmid in the shuttle vector. This is because Pgp1, 2, 6, and 8 are essential for plasmid maintenance, while Pgp3 and 4 are a virulence determinant and regulator of certain chromosomal genes, respectively (31–33). Compared to the native chromosomal *grgA* allele containing a Targetron-insertion site between nucleotides 67 and 68 (Fig. 1A top), the *grgA* allele in pGrgA-DOPE carries a His-tag sequence and four synonymous point mutations around the intron-targeting site (Fig. 1A middle), rendering peig resistant to the Targetron designed for this site. Since ATC-induced GrgA overexpression previously caused *C. trachomatis* growth inhibition (14, 34), we employed a weakened ribosomal binding site identified via a green fluorescence protein reporter (Fig. S2A through D) in pGrgA-DOPE to drive the expression of His-tagged GrgA (His-GrgA). We also removed a region that contained potential alternative −35 and −10 promoter elements between the ATC-inducible promoter and the ribosomal binding site from pGrgA-DOPE (Fig. S2E).

We transformed wild-type *C. trachomatis* L2 bearing an intact chromosomal *grgA* (i.e., L2/cg) with pGrgA-DOPE to derive L2/cg-peig. Western blotting demonstrated comparable amounts of His-GrgA and endogenous GrgA at 12 h postinoculation (hpi) in L2/cg-peig cultures containing 0 to 5 nM ATC (Fig. S3A). We also analyzed the growth of L2/cg-peig in the presence of 0 or 1 nM ATC and found that ATC-induced GrgA overexpression did not affect the expression level of mKate2 [a red fluorescence protein encoded by pGrgA-DOPE (Fig. S1)], the inclusion size, chlamydial chromosome replication kinetics, or progeny EB production (Fig. S3B through F). These findings indicate that we can induce recombinant GrgA expression from pGrgA-DOPE at normal physiologic levels without adverse effects, thereby increasing the likelihood that we will be able to compensate for the loss of endogenous GrgA following the experimental disruption of the endogenous chromosomal *grgA* allele.

We next transformed L2/cg-peig with the aforementioned Targetron plasmid carrying an *aadA*-containing group II intron that targets the insertion site between nucleotides 67 and 68 in *grgA* (Fig. S2). ATC was employed to induce GrgA expression from pGrgA-DOPE while selecting for chromosomal mutants carrying an intron-disrupted *grgA* using spectinomycin. PCR analysis confirmed the genotypes of L2/cg, L2/cg-peig, and the plasmid-complemented, chromosomal *grgA*-*aadA*-disrupted L2/cgad-peig (Fig. 1A and B;

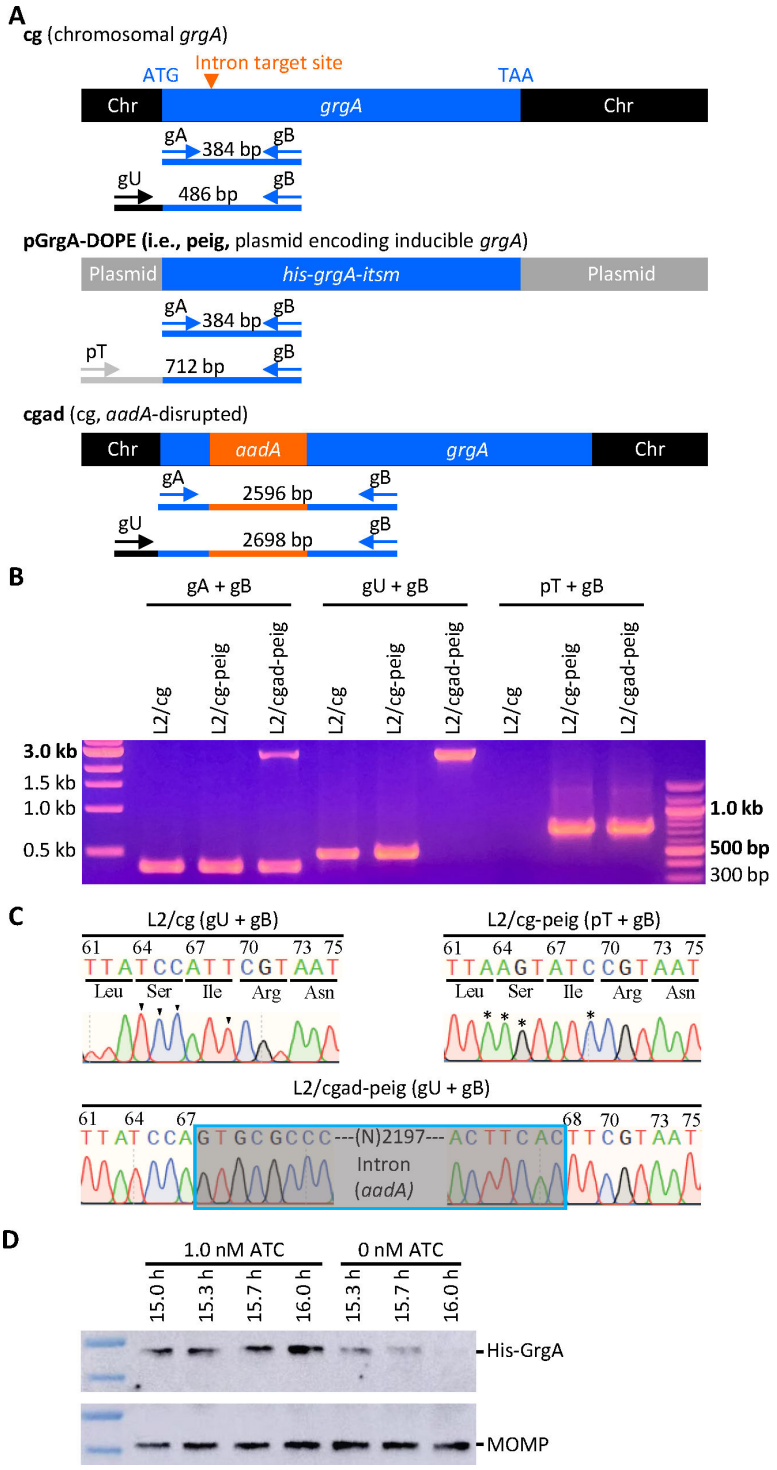

FIG 1 Confirmation of the disruption of the chromosome-encoded *grgA* by group II intron and re-expression of GrgA from a transformed plasmid in the DOPE system. (A) Schematic drawings of *grgA* alleles, locations of intron target site, diagnostic primers, and sizes of PCR products obtained with different sets of primers. Abbreviations: itsm, intron target site mutated; Chr, chromosome. (B) Gel image of PCR products amplified with DNA of wild-type *C. trachomatis* L2 with intact chromosomal *grgA* (L2/cg), L2/cg transformed with the *his-grgA-itsm* expression plasmid pGrgA-DOPE (L2/cg-peig), and L2 with *aadA*-disrupted chromosomal *grgA* complemented with pGrgA-DOPE (L2/cgad-peig) using primer sets shown in (A). (C) Sanger sequencing tracings of PCR products showing the intron target site in

(Continued on next page)

FIG 1 (Continued)

L2/cg, mutations surrounding this site conferring resistance to intron targeting in peig, and *grgA*-intron joint regions in the chromosome of L2/cg-peig. Wild-type bases and corresponding mutated bases are shown with arrowheads and asterisks, respectively. (D) Western blotting showing time-dependent loss of His-GrgA in L2/cgad-peig upon ATC withdrawal. HeLa cells infected with L2/cgad-peig were cultured in the presence of 1 nM ATC. Three cultures were switched to ATC-free medium at 15 h postinoculation hpi. Cultures were harvested with SDS-PAGE sample buffer at indicated times and resolved by SDS-PAGE. The membrane was first probed with mouse monoclonal MC22 anti-major outer membrane protein (MOMP) antibody, striped, and then reprobed with a polyclonal rabbit anti-GrgA antibody.

Table S1). Sanger sequencing confirmed the nucleotide sequences surrounding the intron target site in L2/cg and L2/cg-peig, and the *grgA*-intron joint regions in L2/cgad-peig (Fig. 1C). Importantly, western blotting detected a time-dependent GrgA loss in L2/cgad-peig following ATC withdrawal (Fig. 1D). By 2 h post-ATC withdrawal, His-GrgA was nearly undetectable. Collectively, the data shown in Fig. 1B through D demonstrate the successful disruption of chromosomal *grgA* in L2/cgad-peig, in which expression, and thus function, of GrgA depends on ATC-induced GrgA expression from pGrgA-DOPE.

GrgA-deficient chlamydiae display slower RB growth and fail to form progeny EBs

To examine the impact of GrgA deficiency on *C. trachomatis* growth and development, we compared the growth of L2/cgad-peig in media with and without 1 nM ATC. Interestingly, immunofluorescence imaging using a major outer membrane protein (MOMP)-specific antibody revealed slower growth in ATC-free cultures as indicated by significantly smaller inclusions (Fig. 2A). Quantitative PCR analysis further confirmed the slower growth in GrgA-deficient cultures as revealed by slower chromosome replication in the absence of ATC (Fig. 2B; Fig. S3). The chromosome doubling time of L2/cgad-peig in the presence of ATC was 2 h (Fig. 2B), identical to the previously reported doubling time of wild-type L2 (14). In contrast, the doubling time of L2/cgad-peig in the absence of ATC doubled to 4 h (Fig. 2B). Intriguingly, ATC-free cultures exhibited a drastic reduction in the production of infectious progeny EBs (Fig. 2C). On average, each ATC-containing culture produced $>10^5$ inclusion-forming units (IFUs) at 24 hpi, near 10^7 at 34 hpi, and $>10^8$ at 48 and 72 hpi (Fig. 2C). By stark contrast, ATC-free cultures produced no detectable IFUs at 24 hpi and only about 300 s EBs at 34 h and thereafter (Fig. 2C). The severe decrease in EB production occurred despite chlamydial chromosome copy number in the ATC-free cultures at 34 hpi being equivalent to that in the ATC-containing cultures at 24 hpi (Fig. 2B). Consistent with the EB quantification assays, ultra-thin section transmission electron microscopy (EM) readily detected EBs and intermediate bodies (IBs) at 35 and 45 hpi in the ATC-containing cultures, whereas EBs were undetectable and IBs were nearly undetectable at 35, 45, or 60 hpi (Fig. 3A) in the ATC-free cultures. Collectively, these results demonstrate a requirement for GrgA for optimal RB growth and the production of EBs.

tetR mutations enable GrgA expression and EBs to escape in the absence of ATC

Although ATC-free L2/cgad-peig cultures exhibited a near complete deficiency in EB formation, we were still able to detect a very low background level of EB production (Fig. 2C). Unlike parental L2/cgad-peig, EBs collected from the ATC-free cultures (i.e., eL2/cgad-peig) grew in subsequent ATC-free cultures as efficiently as in ATC-containing cultures, as evidenced by the morphology of immunostained inclusions (Fig. 4A) and results of IFU assays (Fig. 4B). Based on the inheritable ATC-independent growth exhibited by the escaped EBs, we hypothesized that spontaneous mutations in the *tetR* gene and/or tetO (TetR operator) might impair the *grgA* repression in L2/cgad-peig, thereby allowing for ATC-independent GrgA expression and the production of low levels

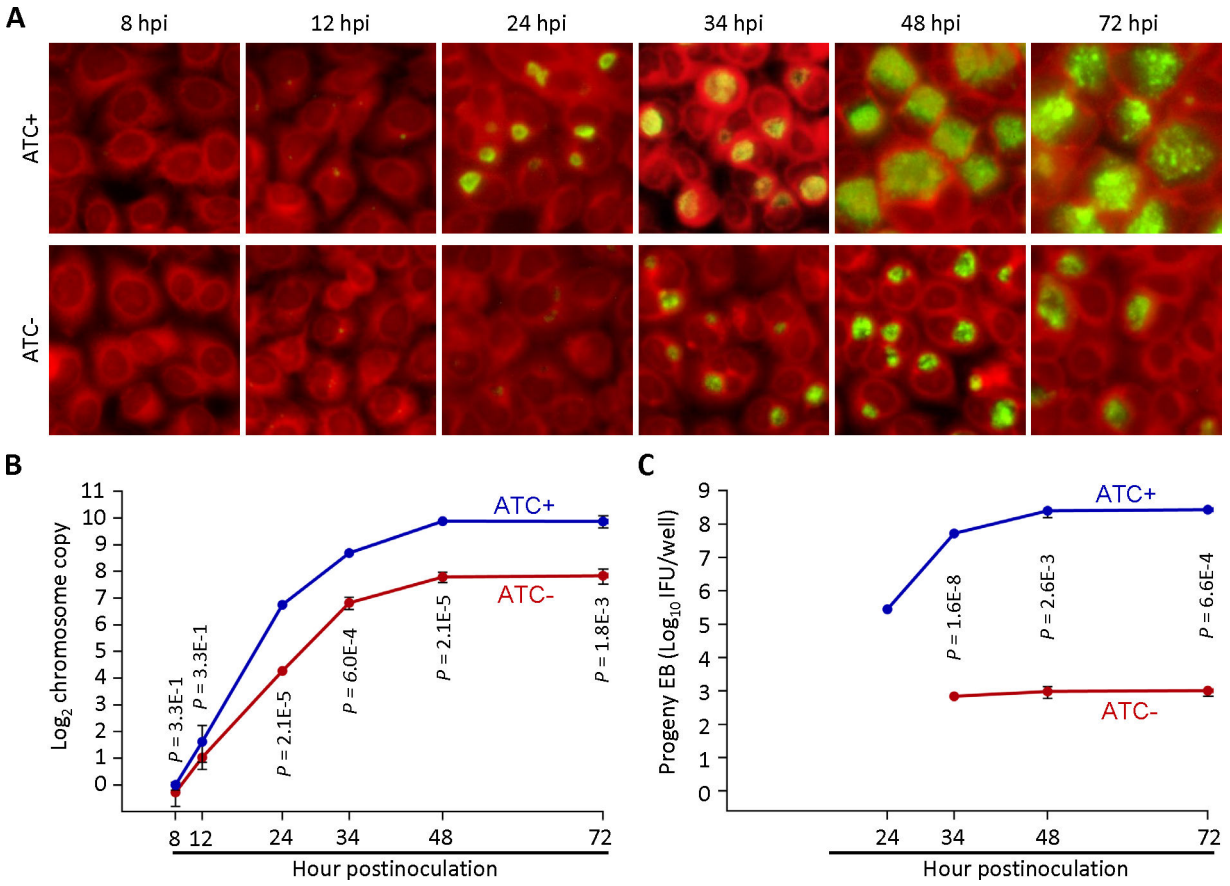

FIG 2 GrgA deficiency slows RB growth and disables the formation of infectious progeny. L2/cg-peig-infected HeLa cells were cultured in the presence or absence of 1 nM ATC. At indicated hpi, cultures were terminated for immunofluorescence assay (A), genome copy quantification (B), or quantification of inclusion-forming unit (C). (A) Infected cells were fixed with methanol, sequentially reacted with monoclonal mouse L2-5 anti-MOMP antibody and a fluorescein isothiocyanate (FITC)-conjugated rabbit anti-mouse IgG secondary antibody, counter-stained with Evan blue, and imaged using a fluorescence microscope. (B) Total genomic DNA, prepared as detailed in Materials and Methods, was used for *C. trachomatis* chromosome quantification by employing primers targeting *ctl0631*. (C) Infected cells were harvested in sucrose-phosphate-glutamate buffer, disrupted by sonication, and inoculated onto monolayers grown on 96-well plates following 10-fold serial dilution. Recoverable inclusion-forming units were detected by immunostaining as described in (A). (B, C) Data represent averages ± standard deviations of triplicate cultures.

of EBs to form in the absence of ATC (Fig. 4C). To test this hypothesis, we first performed western blotting for cells infected with L2/cgad-peig or eL2/cgad-peig. These cells were exposed to ATC-containing medium from 0 to 18 hpi or initially for 16 h, then switched to ATC-free medium for the final 2 h. Notably, ATC withdrawal led to GrgA depletion in L2/cgad-peig but did not alter GrgA expression in eL2/cgad-peig. We further recovered pGrgA-DOPE plasmids from EBs formed in ATC-free cultures. Significantly, DNA sequencing revealed a single nucleotide polymorphism (SNP) in the *tetR* gene in each of the 10 plasmids analyzed. Two of these SNPs lead to premature termination at codons 16 or 158, while the third SNP induces a frameshift at codon 64 (Fig. 4E). These observations support our hypothesis that lack of an authentic TetR results in the unchecked expression of wild-type GrgA in the absence of ATC (Fig. 4C). Together with findings in Fig. 3 and 4, these data further substantiate our supposition that GrgA is necessary for EB production.

GrgA-deficient chlamydiae fail to maintain the virulence plasmid

Fluorescent proteins such as mKate2 are often employed as convenient markers for tracking genetic transformants (35, 36). As depicted in Fig. S3B, L2/cg-peig produced mKate2-positive inclusions in both ATC-containing and ATC-free media. When cultured in

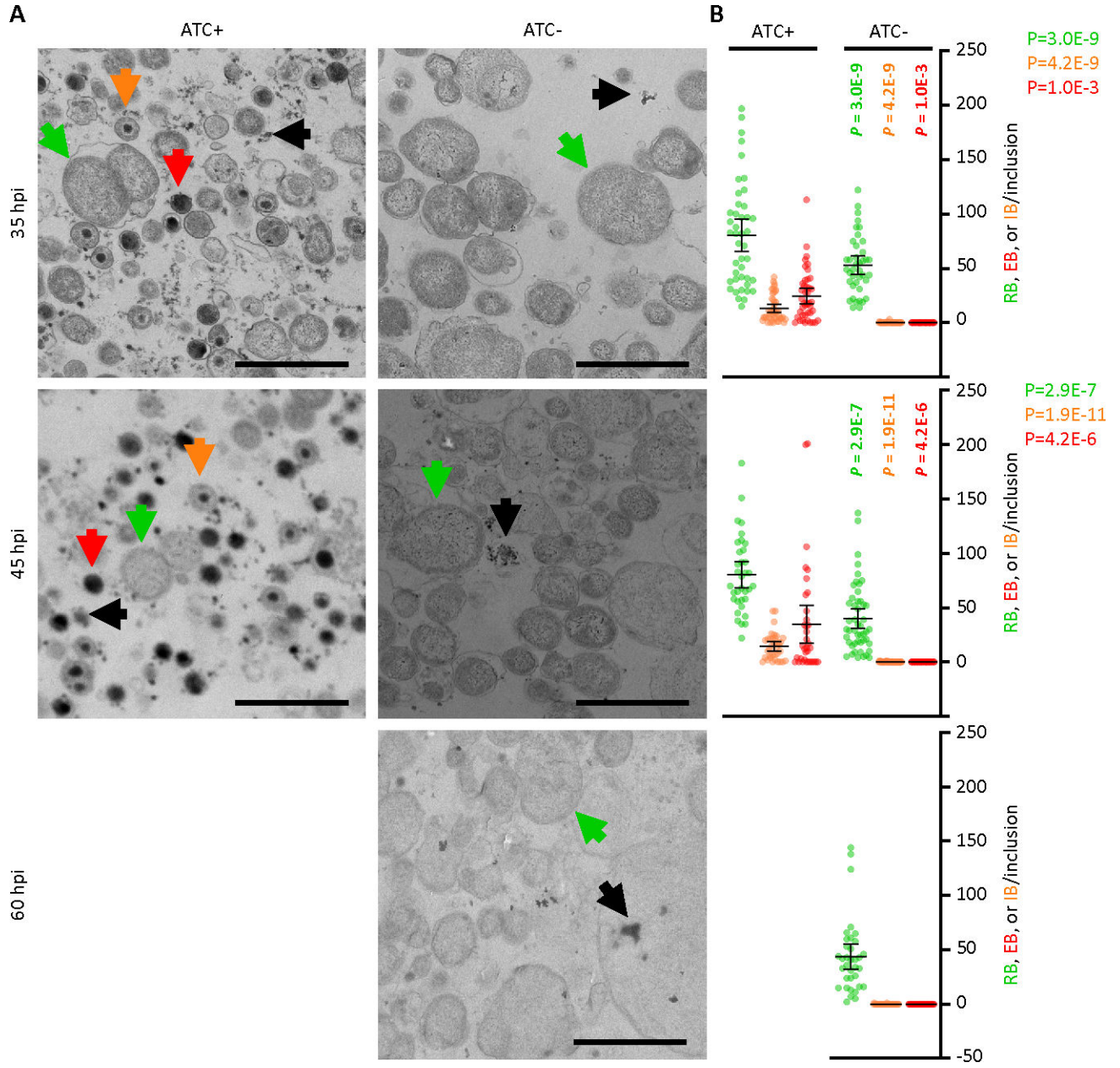

FIG 3 Lack of EB formation in GrgA-deficent cultures. (A) Representative transmission electron microscopic (EM) images of L2/cgad-peig cultured in media containing either 0 nM or 1 nM at indicated hpi. ATC-containing culture was not processed for EM at 60 hpi because nearly all inclusions already burst by that point. Representative RBs, EBs, and IBs are marked by green, red, and orange arrows, respectively. Note that small irregularly shaped electron-dense particles with representative ones pointed to by black arrows, in both ATC-containing and ATC-free cultures, are glycogen particles. Size bar equals 2 µm. (B) Scattergraphs of RBs, EBs, and IBs counted from multiple inclusions.

ATC-containing medium, L2/cgad-peig also displayed mKate2-positive inclusions. However, when cultured in ATC-free medium, the usual mKate2-positive inclusions were largely absent, with only sporadic mKate2 signals observed, as elaborated below.

To analyze these phenomena under higher resolution, we metabolically labeled chlamydiae with a green-fluorescing lipid (N-[7-(4-nitrobenzo-2-oxa-1,3-diazole)]) aminocaproylsphingosine (C6-NBD-ceramide). The metabolic lipid labeling method is based on the host cell's ability to uptake the lipid during the pulse phase and transfer it to the chlamydiae during the chase phase (37, 38). This enables the simultaneous visualization of chlamydiae (depicted in green) and the recombinant plasmid marker

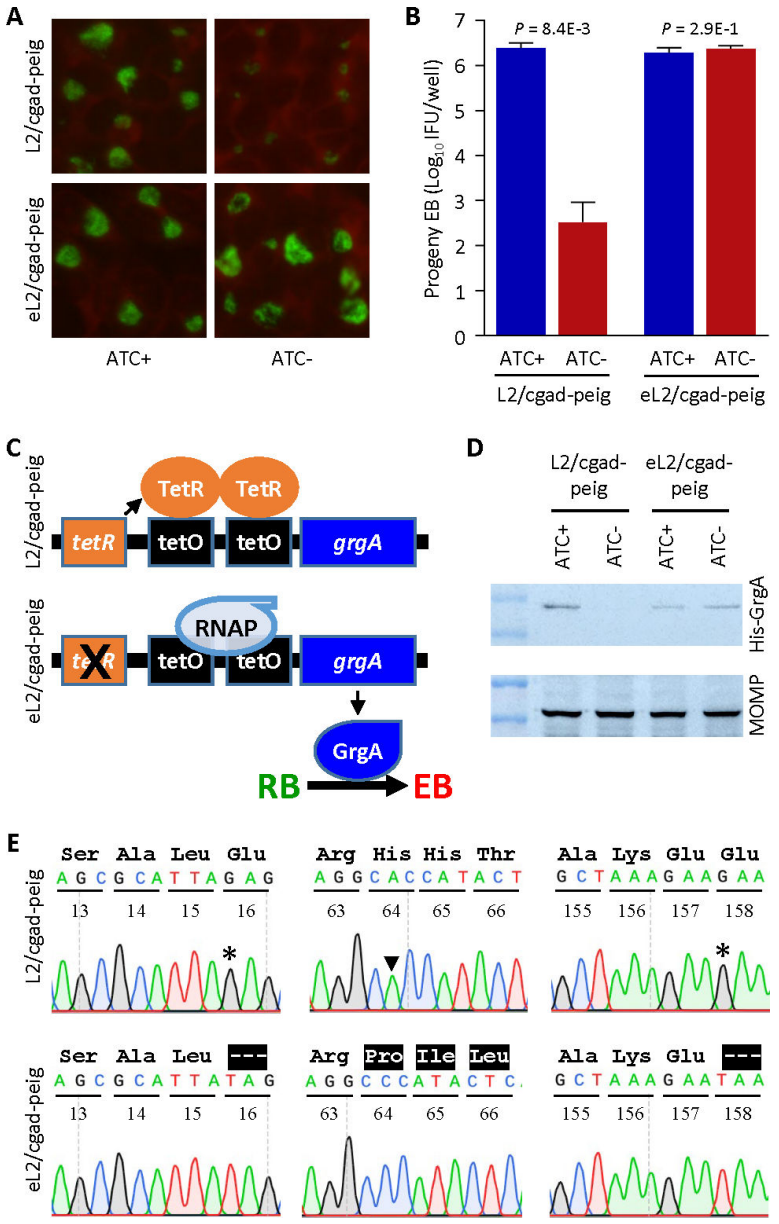

FIG 4 Failed *grgA* repression in pGrgA-DOPE is responsible for EB escape in ATC-free cultures of L2/cgad-peig. (A, B) Escaping L2/cgad-peig (eL2/cgad-peig) was obtained by culturing L2/cagad-peig in ATC-free medium for two passages. eL2/cgad-peig and parental L2/cgad-peig cultured in media containing 0 or 1 nM ATC for 28 h were subject to immunostaining (A) and IFU assays (B) as described in Fig. 2 legend. (C) Schematic shows mechanism for TetR-mediated *grgA* transcription repression in L2/cgad-peig cultured in the absence of ATC (upper) and hypothetical mutations in *tetR* resulting in a loss in TetR-mediated repression, leading to ATC-independent GrgA expression and consequent EB formation (lower). (D) Unlike L2/cgad-peig, GrgA expression in eL2/cgad-peig is independent of ATC. L2/cgad-peig and eL2/cgad-peig were cultured in medium containing 1 nM ATC from 0 through 18 hpi or 0 through 16 hpi, followed by incubation in ATC-free medium for 2 h. Western blotting was performed as described in Fig. 1F legend. (E) Mutations identified in *tetR* in pGrgA-DOPE recovered from L2/cg-peig EBs formed in the absence of ATC lead to premature translation termination or frameshift. Codon positions in *tetR* are numbered. Wild-type amino acid sequences are shown in black. Highlighted hyphens and amino acids indicate protein sequence truncation and alteration, respectively.

mKate (in red) in live cultures using fluorescence microscopy. Because L2/cgad-peig cultures exhibit slower growth in the absence of ATC, and that the number of chromosomes at 24 hpi in ATC-containing cultures is roughly equal to those at 34 hpi in ATC-free cultures (Fig. 2A and B), metabolic lipid labeling was initiated at 17.5 and 27.5 hpi for ATC-containing and ATC-free cultures, respectively, and fluorescence microscopy was conducted at 24 and 34 hpi, respectively.

In ATC-containing but ampicillin-free cultures, almost 100% of inclusions exhibited strong colocalization of green fluorescence lipids and mKate2 signals, as demonstrated by significant color shifts following the merging of the lipid and mKate2 signals (Fig. 5A and B). This indicates widespread plasmid maintenance in chlamydiae. qPCR analysis detected 2.9 to 5.8 plasmids per chromosome (i.e., per cell) during the developmental cycle in ATC-enriched cultures, a count comparable to the native plasmid copy number (4.0 to 7.6 plasmids per chromosome) previously reported for wild-type *C. trachomatis* (39) (Fig. 5C). These findings suggest that L2/cgad-peig, with plasmid-expressed GrgA, is capable of maintaining its virulent plasmid even in the absence of the recombinant plasmid selection agent ampicillin (Fig. S1).

By contrast, in ATC-free cultures, no inclusions exhibiting diffused mKate2 signals of sufficient intensity to allow for significant color shifts upon merging with chlamydial lipid signals were detected (Fig. 5A and B). Indeed, the plasmid per chromosome ratio dropped to 0.5 at 24 hpi, gradually rose to 1.2 by 48 hpi, and remained at this level at 72 hpi (Fig. 5C). These observations imply that GrgA-deficient chlamydiae fail to maintain plasmid copies. Although inclusions in ATC-free cultures do not express diffused mKate2 signals, approximately 20% of the inclusions contained strong, punctate mKate2 signals, hinting at a potential plasmid segregation defect. Notably, ampicillin failed to enhance mKate2 expression (Fig. 5D and E) and only a ~2-fold increase in the plasmid copy number in ATC-free cultures (Fig. 5F), suggesting that the antibiotic that typically selects for the recombinant plasmid under "normal" conditions is unable to maintain the plasmid in the absence of GrgA.

GrgA deficiency leads to insufficient late gene activation

Given that GrgA is a transcriptional activator and that GrgA-deficient RBs fail to differentiate into EBs, we hypothesized that presumptive GrgA regulatory target genes crucial for EB formation may not be adequately activated in GrgA-deficient RBs. To identify these regulatory target genes, we performed RNA-Seq analysis on L2/cgad-peig cultured with and without ATC. We conducted RNA-Seq for ATC-containing cultures at 18 hpi and 24 hpi, corresponding to the midcycle point and early late developmental cycle point, respectively, in L2/cgad-peig (Fig. 2B and C), as well as wild-type *C. trachomatis* (6, 14, 34). Considering the slower growth rate of L2/cgad-peig cultured in ATC-free medium (Fig. 3), we extended the culture time to 24 hpi and 36 hpi before extracting RNA. qPCR analysis confirmed that chromosome copy numbers in ATC-containing cultures at 18 hpi were the same as those in ATC-free cultures at 24 hpi, while chromosome copy numbers of ATC-containing cultures at 24 hpi were comparable to those of ATC-free cultures at 36 hpi (Fig. 6A).

We obtained on average of 6.3 million RNA-Seq reads mapping to the *C. trachomatis* genome per sample, representing 600 times genome coverages. Principal component analysis revealed strong consistencies within biological triplicates but notable differences among groups based on culture conditions and developmental stages (Fig. 6B). Consistent with the GrgA protein expression data in Fig. 1D and plasmid copy number data (Fig. 5C), RNA-Seq detected 204- and 157-fold decreases in the transcripts of *his-grgA* encoded by pGrgA-DOPE in the ATC-free cultures of L2/cgad-peig at the corresponding midcycle and early late developmental points, respectively, compared with ATC-containing cultures (Table S1).

We identified 150 genes activated by 2- to 56-fold ($P \leq 0.05$) in ATC-containing cultures from 18 hpi (midcycle) to 24 hpi (early late stage) (Table S2). Most likely, these late genes either drive or are consequent to the conversion of RBs into EBs. Indeed, the top two

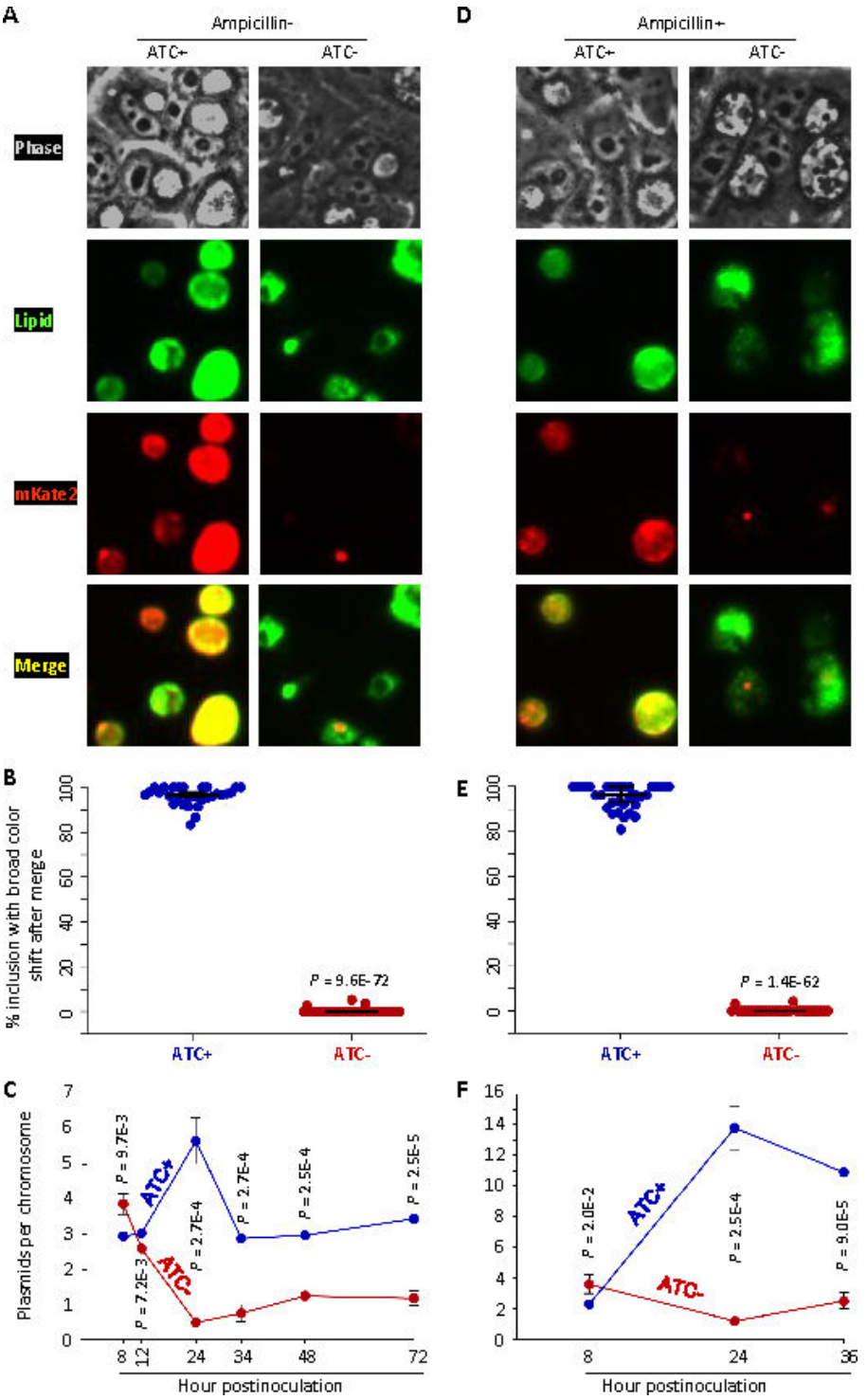

FIG 5 GrgA deficiency causes plasmid loss. (A, B) L2/cgad-peig cultured with ampicillin-free media containing 0 nM or 1 nM ATC was metabolically labeled with the fluorescent lipid C6-NBD-ceramide as described in Materials and Methods. C6-NBD-ceramide-labeled *Chlamydia* (green) and mKate expressed from the plasmid are imaged under a fluorescence microscope. (A) Representative images of live cultures of L2/cgad-peig labeled with C6-NBD-ceramide. Note that the red fluorescence protein mKate2 is expressed by pGrgA-DOPE, which also encodes a β-lactamase rendering ampicillin resistance. (B) Scattergraph of percentages of inclusions with broad color shift after merging green and red channels from multiple images from cultures described in A. (C) Kinetics of plasmids per chromosome in L2/cgad-peig cultured with ampicillin-free media containing 0 nM or 1 nM ATC. Total DNA was prepared at indicated times. qPCR analysis was performed for the

(Continued on next page)

FIG 5 (Continued)

chromosomal gene *ctl0631* and the plasmid gene *pgp1*. The plasmid/chromosome ratio was derived as described in Materials and Methods. Quantification of the pGrgA-DOPE and chromosome was carried out with qPCR as described in Materials and Methods. Data represent averages ± standard deviation from biological triplicates. (D, E) L2/cgad-peig cultured with 0 nM or 1 nM ATC plus 10 µg/mL ampicillin was metabolically labeled with the fluorescent lipid C6-NBD-ceramide. (D) Representative images of live cultures of L2/cgad-peig labeled with C6-NBD-ceramide with or without 1 nM ATC. (E) Scattergraph of percentages of inclusions with broad color shift after merging green and red channels from multiple images from cultures described in A. (F) Kinetics of plasmids per chromosome cultured with 0 nM and 1 nM ATC plus 10 µg/mL ampicillin as determined in panel C.

ranked genes encode an EB-enriched cysteine-rich outer membrane protein OmcA and a histone HctB, both essential for EB morphogenesis. When changes of these 155 late genes in the ATC-free cultures from 24 hpi (midcycle) to 36 hpi (early late stage) were plotted alongside the ATC-containing cultures (Table S2), it was notable that 43 of the 45 genes with ≥5-fold expression increases in the ATC-containing cultures failed to increase to the same degree in the ATC-free cultures (Fig. 6C; Table S2). For example, *hctB* increased 41.2-fold in ATC-containing cultures but only 5.3-fold in ATC-free cultures. *omcA* increased 56.2-fold in ATC-containing cultures but only 21.1-fold in ATC-free cultures (Fig. 6C; Table S2). Similarly, *omcB* increased 20.5-fold in ATC-containing cultures but only 4.9-fold in ATC-free cultures (Fig. 6C; Table S2). The protease-encoding gene *tsp*, thought to degrade certain RB-specific proteins toward the end of midcycle (40), exhibited a 5.5-fold increase in ATC-containing cultures but only a 1.7-fold increase in ATC-free cultures (Fig. 6C; Table S2). Results of quantitative reverse transcription-PCR (qRT-PCR) analysis demonstrated consistent increases in *omcA, omcB, hctB,* and *tsp* in ATC-containing cultures but not in ATC-free cultures from midcycle to early late cycle (Fig. 6D). These findings support the notion that GrgA is critical for adequate activation of late genes involved in the RB-to-EB conversion.

A direct comparison of RNA-Seq data from ATC-containing and ATC-free cultures of L2/cgad-peig obtained at the early late developmental point (Fig. 6A) highlighted 64 chromosomal genes that were downregulated by 2.0- to 9.1-fold in ATC-free cultures (Table S3). As expected, the aforementioned *hctB, omcA, omcB,* and *tsp* are included in these 63 genes. Among the remaining genes, many encode T3SS structure (e.g., *copB, copD*), effector (e.g., *tarp*), or chaperone proteins (e.g., *scc2*). In late developmental stages, some T3SS effectors are secreted to enable chlamydial exit from host cells (e.g., CTL0480 and CTL0481), while other effectors are not secreted until EBs enter new host cells in the next developmental cycle (e.g., TARP) (29, 30, 41–45). These findings suggest that GrgA not only is essential for EB formation but also plays important roles in the dissemination of progeny EBs.

RNA-Seq detected a higher *hctA* expression increase in ATC-free cultures than in ATC-containing cultures from the midcycle to the early late developmental point, compared to a reduced *hctB* expression increase (Fig. 6C; Table S2). However, qRT-PCR analysis revealed similar *hctA* expression increases in ATC-free and ATC-containing cultures between the two developmental points (data not shown). This suggests that GrgA does not regulate *hctA* expression.

GrgA deficiency downregulates expression of target genes of σ28 and σ54

Our previous *in vitro* study showed that GrgA can directly activate transcription from σ28-dependent promoters in addition to σ66-dependent promoters (15). Notably, the aforementioned *hctB* and *tsp* downregulated in ATC-free cultures of L2/cgad-peig at early late developmental points constitute the entire σ28 regulon (46). This *in vivo* observation confirms that GrgA regulates the expression of σ28 genes in *Chlamydia*.

Two research groups have proposed partially overlapping gene sets as the σ54 regulon in *C. trachomatis*. While Soules et al. suggested 64 targets through overexpression of the σ54 activator *atoC* (*ctcC*) (11), Hatch et al. proposed nearly 30 targets through σ54 depletion (46). Significantly, of the 64 genes exhibiting ≥2-fold decreases in ATC-free

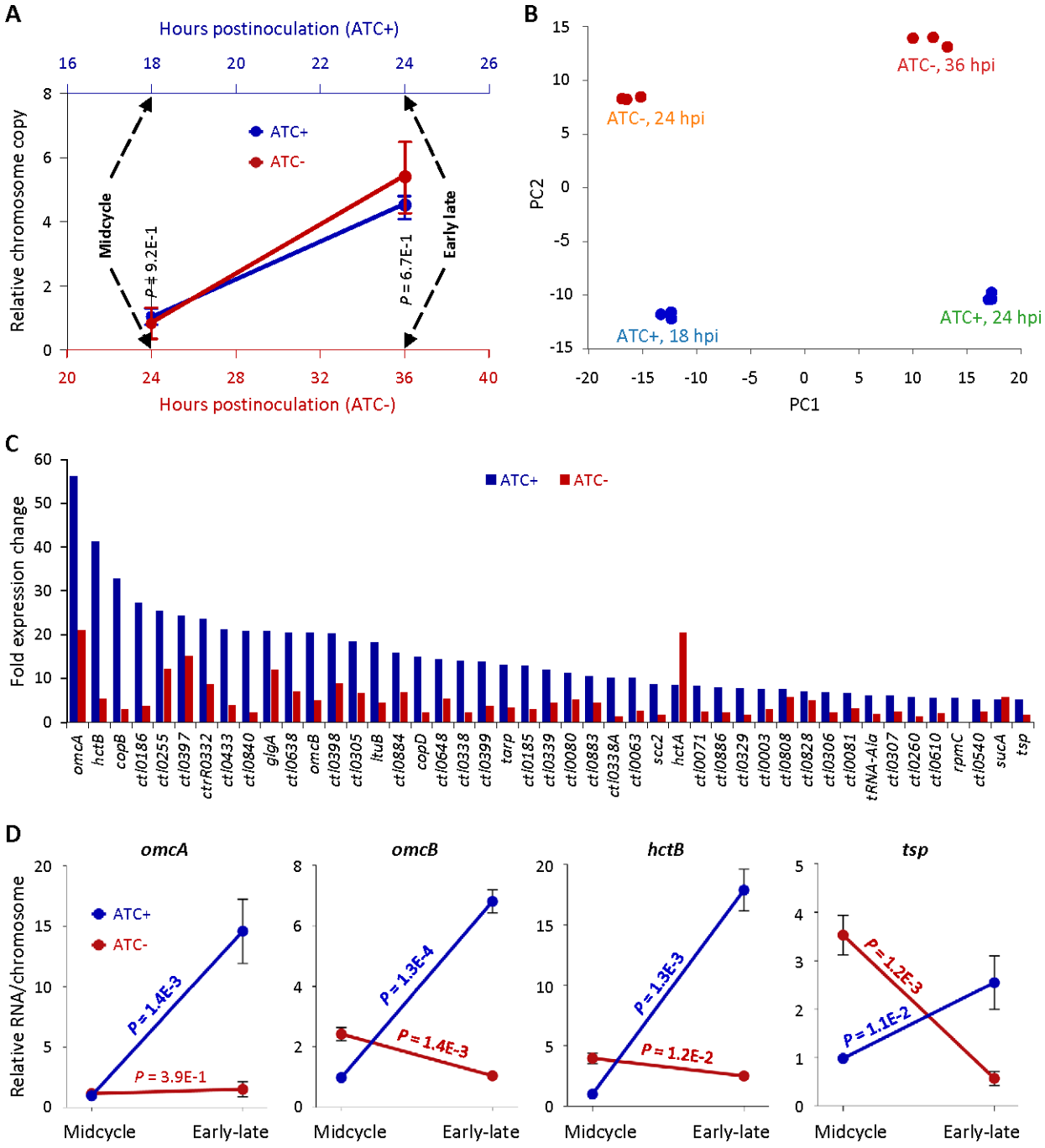

FIG 6 GrgA deficiency disrupts late gene activation. RNA and DNA were prepared from L2/cgad-heig and were cultured with 0 nM or 1 nM ATC. (A) Timing of RNA extraction for RNA-Seq analysis of ATC-containing and ATC-free cultures of L2/cgad-peig and equivalent chromosome copies in two types cultures at the defined midcycle points as well as the early late cycle points. (B) High intragroup consistency of RNA-Seq data revealed by principal component analysis. (C) Most of late genes with ≥5-fold increases in ATC-containing cultures had lower degree of increases in ATC-free cultures in RNA-Seq analysis. (D) Confirmation of insufficient activation of four late genes in ATC-free cultures by quantitative reverse transcription-PCR analysis. Data were averages ± standard deviations of biological triplicates.

cultures, 42 genes, including the aforementioned *omcA, omcB, hctB*, and numerous T3SS-related genes, are σ54 targets proposed by either or both studies (Table 1). These observations suggest that GrgA also regulates the expression of σ54 genes.

We noticed moderate (about 1.5-fold) yet significant decreases in transcripts of *rpoN* (σ54), *atoC* (*ctcC*), and *atoS* (*ctcB,* a sensor kinase gene cotranscribed with *atoC*) in

TABLE 1 σ54 targets downregulated by GrgA deficiency at early late developmental points[a]

Gene name	Product description	GrgA-	Soules et al.	Hatch et al.
ctl0338A	Putative T3SS secreted protein	−9.07	DT	
ctl0840	Putative cytosolic protein	−8.42	IT	
ctl0338	Putative T3SS effector	−7.07	DT	
copB	T3SSs translocator CopB	−6.87	IT	T
ctl0329	Putative outer membrane protein	−6.77	IT	
ctl0339	Phosphatidylcholine-hydrolyzing phospholipase D (PLD) protein	−6.57	DT	
ctl0397	T3SS exported protein	−6.55	DT	
tarp	Translocated actin-recruiting phosphoprotein	−6.30	IT	T
scc2	T3SS chaperone	−6.29	IT	T
ctl0305	Secreted, Pmp-like protein	−5.58	DT	
ctl0398	T3SS exported protein	−5.14	DT	
copD	T3SS translocator CopD	−5.07	IT	T
ctl0063	T3SS effector	−5.02	IT	T
ctl0433	Putative exported protein	−4.95	IT	
ctl0071	Hypothetical protein	−4.90	DT	
glgA	Glycogen synthase	−4.89	IT	
ctl0307	Putative secreted, Pmp-like protein	−4.71	DT	
ctl0219	Putative T3SS effector	−3.96	DT	
ctl0220	T3SS secreted protein	−3.61	IT	
ctl0186	Putative membrane protein	−3.56	DT	
hctB	Histone-like protein 2	−3.36	IT	T
ctl0648	Hypothetical protein	−3.36	IT	
ctl0080	Putative T3SS effector	−3.18	DT	
ctl0306	Secreted, Pmp-like protein	−3.10	DT	
omcA	Membrane protein	−3.07	DT	T
ctl0209	Putative inclusion membrane protein	−3.02	IT	
glgC	Glucose-1-phosphate adenylyltransferase	−3.01	DT	T
ctl0883	Putative T3SS effector	−2.90	DT	
ctl0610	Thioredoxin domain-containing protein	−2.80	IT	
ctl0221	T3SS secreted protein	−2.74	IT	
ctl0185	Putative membrane protein	−2.67	DT	
ctl0081	T3SS effector protein	−2.67		T
tsp	Tail-specific protease	−2.66		T
ctl0540	Putative inclusion membrane protein	−2.57	IT	
ctl0003	Putative T3SS chaperone	−2.53	DT	
omcB	Outer membrane protein OmcB	−2.46	DT	T
ctl0884	Putative T3SS effector	−2.45	DT	
ctl0255	T3SS effector	−2.26	DT	
ctl0260	Inclusion membrane protein	−2.24	DT	
ctl0021	Hypothetical protein	−2.07	DT	
ctl0638	Hypothetical protein	−2.07	IT	
ctl0466	Inclusion membrane protein	−2.06		T

[a]Abbreviation, DT and IT, direct targets and indirect targets, respectively, defined by Soules et al. through RNA-Seq analysis of atoC-overexpressing chlamydiae, promoter sequence analysis, and transcription report assays in *Escherichia coli* (11). T, targets defined by Hatch et al. through RNA-Seq analysis of σ54-depleted chlamydiae (46).

ATC-free cultures of L2/cgad-peig at the early late developmental point. We performed qRT-PCR analysis and confirmed that all these three genes showed significant ≥2-fold decreases (Fig. 7). These observations suggest that GrgA regulates the expression of σ54

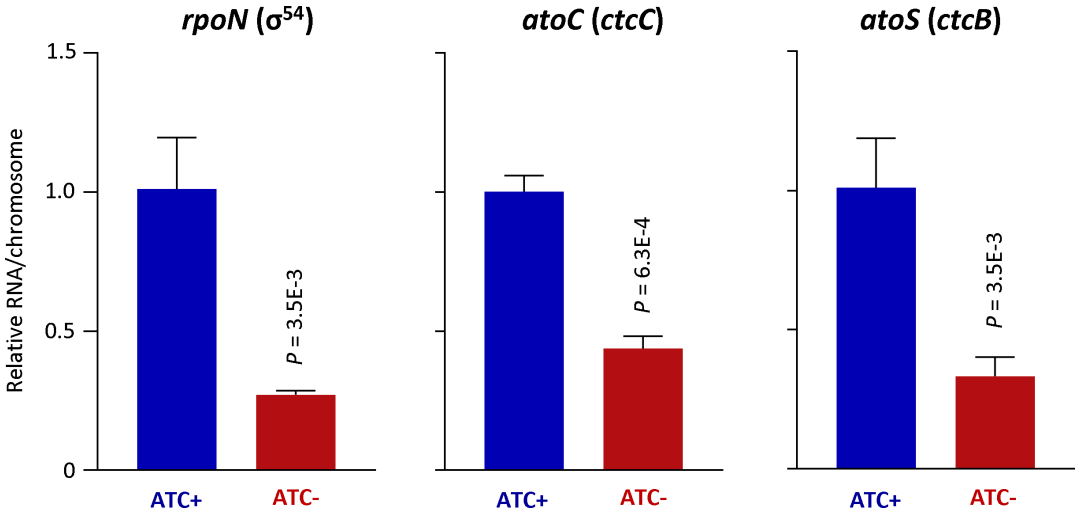

FIG 7 Confirmation of downregulated expression of *rpoN* and its regulators *atoC* and *atoS*. RNA from Fig. 6 was used for qRT-PCR analysis. Data were averages ± standard deviations of biological triplicates.

genes by controlling the expression levels of σ54 and its regulators of *atoC* (*ctcC*) and *atoS* (*ctcB*).

GrgA deficiency disrupts the midcycle transcriptome

Our discovery of early late stage transcriptomic changes underlying EB formation deficiency prompted us to examine midcycle transcriptomic differences in L2/cgad-peig cultures with and without ATC, to further discern the mechanisms by which GrgA regulates RB growth. A total of 28 chromosomal genes exhibited a 2.0- to 4.1-fold downregulation ($P < 0.05$) in ATC-free L2/cgad-peig cultures as determined by RNA-Seq. Interestingly, of these 28 chromosomal genes, 7 (25%) encode tRNAs (Table 2). Of note, 10 other tRNA genes displayed 1.5- to 2.0-fold decreases ($P < 0.05$, Table S1). Together, these 17 tRNAs constitute nearly half of the 37 tRNAs expressed in *C. trachomatis*, thus suggesting that GrgA supports RB growth in part, by boosting tRNA expression and protein synthesis.

Among the remaining 21 chromosomal genes with ≥2.0-fold expression decreases in ATC-free L2/cgad-peig cultures during the midcycle, *oppD* and *oppF* encode oligopeptide ABC transporter ATP-binding proteins, while *ctl0674* encodes a metal ABC transporter, and *trpB* encodes tryptophan synthase B. These changes suggest that GrgA promotes RB growth by upregulating both nutrient acquisition from host cells and *de novo* tryptophan biosynthesis, which are both important for chlamydial growth (47, 48).

Two additional genes of interest that are downregulated in ATC-free cultures of L2/cgad-peig during the midcycle are *obgE* and *nth*, which encode DNA topoisomerase IV subunit B and endonuclease III, and are required for DNA replication and repair, respectively. These data suggest that GrgA plays a potential role in the regulation of DNA replication and repair during RB growth.

Interestingly, 70 chromosomal genes showed 2.0- to 5.3-fold increases in ATC-free cultures at the midcycle ($P < 0.05$) compared with ATC-containing cultures (Table S4). The number of upregulated genes is 2.5-fold higher than the number of downregulated genes discussed above (Table 1). This finding raises the possibility that GrgA also functions to regulate the silencing of large networks of developmental genes. Most notably, two well-characterized transcription factors, *euo* (late gene repressor) and *hrcA* (heat-inducible transcriptional repressor), demonstrated aberrantly increased expression in the ATC-free cultures during the midcycle (Table S4). The increased expression of *euo* and *hrcA* was surprising because previous studies found that GrgA overexpression also increased euo and hrcA expression (14). qRT-PCR analysis confirmed that both *euo*

TABLE 2 Midcycle genes downregulated by GrgA deficiency

Gene name	Product description	Fold change	*P*-value
ctl0397	T3SS exported protein	−4.09	1.3E-31
tRNA-Pro	tRNA-Pro	−3.02	3.3E-08
ctl0751	Hypothetical protein	−2.94	1.2E-13
glgA	Glycogen synthase	−2.85	4.7E-75
ctl0009	Rod shape-determining protein MreC	−2.76	6.4E-57
trpB	Tryptophan synthase subunit beta	−2.76	3.0E-37
ctrR12_n	ctrR12_n	−2.59	6.4E-15
tRNA-Leu	tRNA-Leu	−2.48	3.9E-04
ctl0339	Phosphatidylcholine-hydrolyzing phospholipase D (PLD) Protein	−2.43	1.8E-12
ctl0674	Metal ABC transporter permease	−2.38	1.0E-29
nth	Transcription termination/antitermination protein NusA	−2.37	1.5E-14
tRNA-Ile	tRNA-Ile	−2.36	9.6E-10
oppF	Oligopeptide ABC transporter ATP-binding protein	−2.26	1.9E-15
ctl0016	Putative membrane protein	−2.25	4.7E-28
oppD	Oligopeptide ABC transporter ATP-binding protein	−2.25	8.7E-26
ctl0398	T3SS exported protein	−2.24	1.1E-13
ctl0548	Hypothetical protein	−2.22	1.7E-33
ctl0479	Inclusion membrane protein	−2.16	1.3E-08
ctl0614	Hypothetical protein	−2.14	2.8E-11
tRNA-Gly	tRNA-Gly	−2.13	1.3E-02
tRNA-His	tRNA-His	−2.11	8.8E-06
ctl0045	Protein-arginine kinase activator protein	−2.09	1.9E-13
ctl0480	Inclusion membrane protein	−2.08	1.1E-09
ctl655a	ncRNA	−2.07	8.3E-107
ctl0529	Hypothetical protein	−2.04	5.7E-05
tRNA-Arg	tRNA-Arg	−2.03	1.3E-02
obgE	DNA topoisomerase IV subunit B	−2.03	3.8E-30
ctl0305	Secreted, Pmp-like protein	−2.02	6.1E-13
tRNA-Ser	tRNA-Ser	−2.01	5.7E-09

and *hrcA* were indeed increased in ATC-free cultures of L2/cgad-peig (Fig. S4). These findings strengthen the notion that GrgA serves as a master transcriptional regulator in *Chlamydia*.

Although RB replication is apparently inhibited in the absence of GrgA, we observed that four genes involved in DNA replication and repair showed increased expression in ATC-free cultures of L2/cgad-peig during the midcycle time point. These include *ruvB* (Holliday junction DNA helicase RuvB), *recA* (recombinase A), *ihfA* (DNA-binding protein Hu), and *ssb* (single-stranded DNA-binding protein). Intriguingly, all four genes are also upregulated when chlamydial growth is halted in response to heat shock (49), thus suggesting a potential regulatory role for GrgA in modulating environmental stress responses in *Chlamydia*. Similarly, four protease genes (*lon, htrA, ftsH*, and *ctl0301*), four protein chaperone genes (*clpB, clpC, groEL*, and *groES*), and two enzymes that regulate disulfide bonding in proteins (*ctl0152* and *trxB*) also displayed increased expression in ATC-free cultures during the midcycle. In addition to the aforementioned tRNA downregulation, the upregulated protease, chaperone, and disulfide isomerase genes likely contribute to protein homeostatic imbalance and functional impairment, resulting in RB growth inhibition.

Taken together, midcycle RNA-Seq data suggest that GrgA promotes RB growth by optimizing the expression of tRNAs and certain nutrient transports. Furthermore, GrgA may function as both a transcriptional activator and a transcriptional repressor, as discussed below.

Pgp4 target genes are downregulated in GrgA-deficient chlamydiae at the early late developmental point

Through microarray analysis of wild-type *C. trachomatis* as well as variants without a recombinant plasmid or with a plasmid either carrying or not carrying pgp4 at 24 hpi, Song et al. identified Pgp4 as a positive transcriptional regulator of nine chromosomal genes (32). At the early late developmental stage, GrgA deficiency had effects on the expression of these chromosomal genes similar to plasmid and Pgp4 deficiencies (Table S5), suggesting that GrgA regulates these genes primarily through maintaining the virulence plasmid. However, this cannot be said for the midcycle developmental stage, as the effects of plasmid and Pgp4 deficiencies on the transcriptome have not yet been studied at that point.

DISCUSSION

DOPE as a valuable tool for study essential gene in *Chlamydia* and other obligate intracellular organisms

Since the first demonstration of reproducible *Chlamydia* transformation using a shuttle vector 12 years ago (35), the research community has leveraged this reverse genetic tool to investigate gene function via ectopic overexpression, insertional mutagenesis, deletion, and other methods (11, 24–30, 50–54). Nonetheless, the lack of effective strategies to disrupt truly essential genes, particularly those whose overexpression is toxic, has hampered research in *Chlamydia* and other biological systems. In this study, we developed a novel, tightly regulated, inducible expression system termed DOPE, which shares similarity with a system recently reported by Cortina *et al* (53). DOPE facilitates the functional examination of an essential gene by permanently disrupting the gene in the chromosome while conditionally depleting the gene products expressed by the complementing plasmid.

The DOPE system represents a convenient and versatile tool for establishing the essentiality of a gene and, at the same time, investigating the gene's underlying functional mechanisms. An advantage of DOPE over recently developed conditional CRISPR interference systems (51, 55) is that gene depletion in DOPE is achieved by omitting ATC, whereas CRISPR interference relies on ATC's presence. The adverse effects of ATC on *Chlamydia* and other bacteria have been mitigated but not entirely eradicated. In fact, it has been documented that chlamydial growth is inhibited with ATC at concentrations ≥20 nM (36). This makes the application of CRISPR interference to chlamydial infection in animal models challenging, as ATC concentrations in tissues and organs are not easily regulated. Furthermore, potential concerns arise about the adverse effects of ATC on the microbiota, as studies have shown that gut microbiota influences chlamydial pathogenesis (56). In addition to ATC independence, chromosomal gene mutants established using DOPE are devoid of potential off-target effects that may occur with CRISPR interference (57).

GrgA as one of the most important regulators of chlamydial physiology

GrgA is an exclusive *Chlamydia*-specific protein with no homologs in non-chlamydial organisms, yet highly conserved among chlamydiae, including environmental chlamydiae (16). By employing the DOPE strategy, we demonstrate that GrgA plays a critical role in sustaining RB replication efficiency and is absolutely essential for RB-to-EB differentiation (Fig. 3 and 4).

RNA-Seq analysis revealed numerous mechanisms through which GrgA regulates RB growth and EB formation. Perhaps chief among these regulatory mechanisms, during

the midcycle, GrgA-deficient RBs exhibited decreased expression of numerous tRNA genes and ABC transporter genes, while displaying increased transcripts of protease genes and chaperone genes (Table S4). These findings suggest that GrgA enables optimal RB growth in part by facilitating RB protein synthesis and nutrient acquisition and by modulating post-translational protein homeostasis. Many other gene expression changes induced by GrgA deficiency (Table 1, Table S1) likely exert additive or synergistic effects on RB growth. In addition to regulating chromosomal gene expression, our findings here show that GrgA may also regulate RB growth by enabling plasmid replication and segregation (Fig. 5). Consistent with this notion, plasmid-free *Chlamydia muridarum* has slower RB replication kinetics (58). Mechanistically, even though Pgp4 has been shown to function as a transcription regulator of chromosomal genes (Table S5) (32, 59), its role in the transcriptomic expression during the midcycle has yet to be investigated.

The morphological signature features of EBs are their small size and high electron density. The RB-to-EB conversion necessitates DNA condensation and reorganization of the chlamydial envelope. These processes involve histones (i.e., HctA and HctB) and outer membrane proteins (e.g., OmcA and OmcB) (2–4), respectively. Significant in this regard, our transcriptomic analysis of the early late developmental stage suggests that GrgA facilitates RB-to-EB differentiation by activating the expression of the histone gene *hctB* and late-stage outer membrane protein genes *omcA* and *omcB*. Moreover, GrgA may aid EB formation by inducing the protease gene *tsp* and modulating numerous other genes (Fig. 6C and D; Tables S1 and S2).

Promoter reporter analysis suggests that *hctA* expression precedes *hctB* (60). Our transcriptomic analysis indicates that GrgA is required for increased expression of *hctB* but not *hctA* at the early late developmental point (Fig. 6C and D; Tables S2 and S3). Despite this, GrgA-deficient RBs fail to produce IBs, a transition cell type during the RB-to-EB conversion (Fig. 3). This finding implies that DNA condensation requires both the actions of both HctA and HctB.

In conjunction with optimizing RB growth and enabling EB formation, our RNA-Seq analysis suggests that GrgA plays additional important roles in the chlamydial developmental cycle. For example, numerous genes encoding T3SS structure proteins, effectors, and chaperones were observed to be downregulated in GrgA-deficient chlamydiae. Among the downregulated genes were the effectors CTL0480 that interacts with the host myosin phosphatase pathway and regulates chlamydial exit (30, 42), and TARP which is secreted from EBs immediately after they are taken up by host cells and interacts with host cytoskeleton protein actin to facilitate cell entry (41, 43, 44). Decreased transcripts of *ctl0480* and *tarp* in GrgA-deficient chlamydiae were observed at the early late developmental stage, thus suggesting that GrgA helps facilitate EB exit from infected cells and invasion of new host cells, both of which are required for chlamydial dissemination.

GrgA as a crucial regulator of chlamydial plasmid maintenance

The plasmids of *C. trachomatis* and *C. muridarum* serve as important virulence factors in these two species (31, 61–63). Our results of lipid metabolic labeling and mKate imaging (Fig. 5) indicate that GrgA plays a crucial role in *C. trachomatis* plasmid replication and/or segregation. The plasmid loss is consistent with an apparent decrease in glycogen particles observed with EM in ATC-free cultures of L2/cgad-peig (Fig. 3A) since Pgp4 is required for efficient *glgA* (glycogen synthesis) expression (Table S5) (32). To the best of our knowledge, other than the standard DNA replication machinery components, GrgA is the first chromosome-encoded regulatory protein required for maintaining the chlamydial plasmid.

The mechanism through which GrgA maintains the virulence plasmid is unclear. Previous studies established that *pgp1, pgp2, pgg6,* and *pgp8* are essential for the maintenance of the plasmid. Our qRT-PCR analysis and qPCR analyses demonstrated that the transcript/plasmid ratios for all *pgp* genes are actually higher in ATC-free cultures

than in ATC-containing cultures (data not shown). These findings suggest that plasmid loss in GrgA-deficient chlamydiae is not caused by decreased *pgp* expression.

GrgA as a master transcriptional regulator

As a component of the RNAP holoenzyme, sigma factor recognizes and binds to specific promoter sequences (8, 64, 65). Based on the temporal expression profiles of chlamydial sigma factors and recent studies, it is generally recognized that σ66 is the principal housekeeping sigma factor, whereas σ28 and σ54 regulate the expression of certain late genes regulating the differentiation of RBs into EBs (11, 12, 46, 66). While controversies exist regarding the exact composition of the σ28 and σ54 regulons in *C. trachomatis* (11, 12, 46, 66), numerous previously reported σ28 and σ54 target genes were found to be downregulated by GrgA deficiency (Table 1). These findings indicate that GrgA not only regulates σ66 genes, but also σ28 and σ54 genes.

Previous studies suggest that distinct GrgA domains directly bind to σ66 and σ28 to regulate the expression of their respective target genes (15, 16) (Fig. 8). Among the numerous σ66 target genes are *rpoN* (σ54), *atoC* (activator of σ54), and *atoS* (presumed positive regulator of AtoC). Findings from this study (Fig. 7) indicate that GrgA stimulates the expression of all these three genes to upregulate σ54 target genes (Fig. 8).

In vitro transcription analysis established that GrgA functions as a transcriptional activator (14–16). Surprisingly, *euo* and *hrcA,* whose promoter activities were stimulated by GrgA *in vitro* and whose transcripts were increased by GrgA overexpression, exhibited increased transcripts in GrgA-deficient chlamydiae (Tables S1 and 4; Fig. S4). This seemingly inconsistency raises the possibility that increased *euo* and *hrcA* expression in GrgA-deficient chlamydiae could be the result of indirect regulation. However, the fact that GrgA deficiency resulted in 2.5 times more increased genes (Table S4) than decreased genes (Table S3) during the midcycle raises the possibility that GrgA could function as both an activator and a repressor. It is worth noting that other bacterial transcription factors can both activate and repress genes (67–69). For example, the cyclic AMP receptor protein binds different region of an outer membrane protein promoter and activates transcription by directly interacting with RNAP but can also repress the transcription after recruiting a transcriptional corepressor (67). The transcription factor Fur can either inhibit RNAP binding to the promoters of iron-uptake genes or facilitate its recruitment to other gene promoters (70). We speculate that GrgA could regulate its target genes in an analogous manner. Alternatively, rather than being directly activated by GrgA, some σ66-dependent genes might exhibit enhanced expression as a result of increased availability of σ66-RNAP when GrgA is absent and not directing it to GrgA target genes. Taken together, GrgA regulates the expression of target genes of all three sigma factors, albeit through distinct mechanisms; GrgA also regulates the expression of other transcription factors. These functions validate GrgA's role as a master transcriptional regulator in *Chlamydia*.

In summary, DOPE has enabled us to disrupt an essential chromosomal gene *grgA*. We show that GrgA serves as a checkpoint for chlamydial secondary differentiation and a crucial regulator of RB growth and plasmid maintenance. The formation of EBs is absolutely required for dissemination of chlamydial infection within the infected host and transmission to new hosts. Because RBs and EBs share most of the immunodominant antigens (e.g., major outer membrane protein), conditional GrgA-deficient, "maturation"-defective chlamydiae are potential candidates for live attenuated *Chlamydia* vaccines, provided that strategies are in place to fully prevent EBs from escaping the gene expression regulatory system in DOPE plasmid. To the minimum, the maturation-defective chlamydiae will serve as a useful system for studying the roles of RBs in antichlamydial immunity.

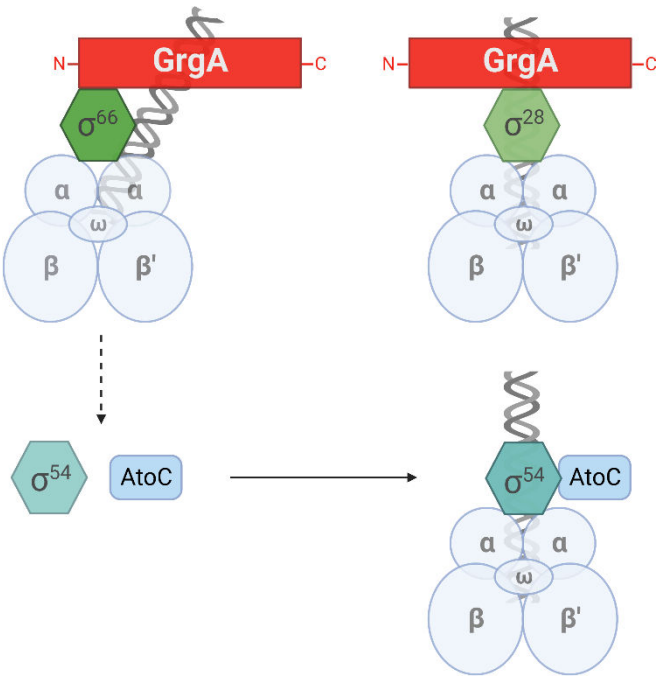

FIG 8 Proposed mechanisms for regulation of σ66, σ28, and σ54 target genes by GrgA. Distinct regions of GrgA interact with σ66 and σ28 to directly regulate the transcription from their target gene promoters by the RNA polymerase core enzyme (comprised of α, β, β′, and ω subunits). Among σ66-dependent genes are *rpoN* (σ54) and *atoC*, which are upregulated by GrgA. Accordingly, σ54 target genes are indirectly upregulated by GrgA. Figure was generated using paid subscription to Biorender.

MATERIALS AND METHODS

Vectors

pTRL2-grgA-67m (Fig. S1), which carried a *grgA* allele with resistance to intron insertion between nucleotides 67 and 68, was constructed by assembling three DNA fragments using the NEBuilder HiFi DNA assembly kit (New England Biolabs). All three fragments were amplified from pTRL2-His-GrgA (34) using Q5 DNA polymerase (New England Biolabs). Fragment 1 was generated using primers pgp3-pgp4-F and His-RBS-R (Table S6). Fragment 2 was generated using primers RBS-His-F and GrgA-67-R (Table S5). Fragment 3 was generated using primers GrgA-67-F and pgp4-pgp3-R (Table S5).

pDFTT3(aadA), a Targetron vector for disrupting chlamydial genes through group II intron insertional mutagenesis (71), was a generous gift from Dr. Derek Fisher (Southern Illinois University, IL). To construct pDFTT3(aadA)-GrgA-67 (Fig. S2), which was designed for disrupting the open reading frame of *grgA*, two PCR fragments were first generated using pDFTT3(aadA) as the template. Fragment 1 was obtained using primers GrgA67_IBS1/2 and the Universal primer (Table S5), while fragment 2 was obtained using primers GrgA67_EBS2 and GrgA67_EBS1/delta (Table S5). The two fragments were combined and subject to PCR extension. The resulting full-length intron-targeting fragment was digested with *Hind*III and *BsrG*I and subject to ligation with *Hind*III- and *BsrG*I-digested pDFTT3(aadA). The ligation product was transformed into *E. coli* DH5α, which was plated onto lysogeny broth agar plates containing 500 µg/mL spectinomycin and 25 µg chloramphenicol. The authenticity of the insert in pDFTT3(aadA)-grgA-67m was confirmed using Sanger sequencing, a service provided by Quintara Biosciences.

Host cells and culture conditions

Mouse fibroblast L929 cells were used as the host cells for *C. trachomatis* transformation and preparation of highly purified EBs. Human vaginal carcinoma HeLa cells were used

for experiments determining the effects of GrgA depletion on chlamydial growth and development. Both L929 and HeLa cell lines were maintained as monolayer cultures using Dulbecco's modified Eagle's medium (DMEM) (Sigma Millipore) containing 5% and 10% fetal bovine serum (vol/vol), respectively. Gentamicin (final concentration: 20 µg/mL) was used for maintenance of uninfected cells and was replaced with penicillin (10 units/mL) and/or spectinomycin (500 µg/mL) as detailed below. 37°C, 5% CO_2 incubators were used for culturing uninfected and infected cells.

Chlamydiae

Wild-type *C. trachomatis* L2 434/BU (L2) was purchased from ATCC. L2/cg-peig was derived by transforming L2 EBs with pTRL2-grgA-67m using calcium phosphate as previously described (34). The transformation was inoculated onto L929 monolayer cells and selected with penicillin as previously described (34). L2/cgad-peig was derived by transforming L2/cg-peig with pDFTT3(aadA)-grgA-67m in the same manner. ATC was added to the cultures immediately after transformation to induce the expression of GrgA from pDFTT3(aadA)-grgA-67m. 12 hours later, spectinomycin D (final concentration: 500 µg/mL) was added to the culture medium to initiate selection (34). L2/cgad-peig EBs were amplified using L929 cells and purified with ultracentrifugation through sequential 35% MD76 density gradient and 40%/44%/52% MD76 gradients (72). Purified EBs were resuspended in sucrose-phosphate-glutamate buffer; small aliquots were made and stored at −80°C. We added cycloheximide to all chlamydial cultures (final cycloheximide concentration in media: 1 µg/mL) to optimize chlamydia growth. Populations of escaping L2/cgad-peig (eL2/cgad-peig) were obtained by culturing L2/cgad-peig without ATC for two or three passages before they were used for growth analysis, western blotting, and plasmid recovery, respectively.

Plasmid extraction from eL2/cgad-peig

Cells in six-well plates were infected with EB to achieve ≥90% infection rate and cultured for 40 hpi. After removal of the medium, 200 µL H_2O was added and cells were removed from the plates with the aid of a Cell Lifter (Corning). The lysate was collected into an Eppendorf tube containing 20 µL of 10× phosphate-buffered saline (PBS) to bring back isotonicity and centrifuged at 3,000 rpm using a Beckman desktop minifuge. The supernatant-containing chlamydial cells were collected and heated at 95°C for 5 min, centrifuged at 14,000 rpm in the minifuge. Plasmids released were purified with phenol/chloroform extraction and precipitated using ethanol. The precipitated DNA was dissolved in 5–10 µL H_2O, which was used to transform *E. coli*.

Immunofluorescence staining

Because chlamydiae are obligate intracellular bacteria, traditional methods used for assessing free-living bacteria growth, such as optical density and agar plate colony-forming unit measurements, are not suitable for determining chlamydial growth. Instead, immunostaining of *C. trachomatis* inclusions is used as a qualitative method to evaluate its growth. Near-confluent HeLa monolayers grown on six-well plates were inoculated with L2/cgad-peig at a multiplicity of infection of 0.3 inclusion-forming units per host cell. Following 20-min centrifugation at 900 *g*, cells were cultured at 37°C in media containing either 0 nM or 1 nM ATC for 30 h. The infected cells were then fixed with cold methanol, blocked with 10% fetal bovine serum prepared in PBS, and stained successively with the monoclonal L21-5 anti-major outer membrane protein antibody (73) and an FITC-conjugated rabbit anti-mouse antibody cells. Immunostained cells were finally counter-stained with 0.01% Evans blue (in PBS). Red (Evan blue) and green (MOMP) fluorescence images were acquired on an Olympus IX51 fluorescence microscope equipped with an Olympus monochrome ICC camera or an Infinity i8-3 CMOS monochrome camera. A constant exposure time for each channel was used for cultures in the same experiments. Overlay of images obtained with the Olympus camera and Infinity i8-3 camera was performed using the PictureFrame software and ACINST03

software, respectively. The Java-based ImageJ software was then used to calculate areas and mKate intensities of inclusions (34).

IFU assay

The IFU assay, which quantifies EBs by determining IFUs in host cells, serves essentially as a chlamydial colony-forming unit assay. Frozen purified L2/cgad-peig EB stock or crude harvests of L2/cgad-peig cultured with or without ATC were thawed, 1-to-10 serially diluted, and inoculated onto L929 monolayers grown on 96-well plates using medium containing 1 nM ATC and 1 µg/mL cycloheximide. Following 20-min centrifugation at 900 *g*, cells were cultured at 37°C for 30 h. Cell fixation and antibody reactions were performed as described above. Immunostained inclusions were counted under the fluorescence microscope without Evan blue counter-staining.

Diagnostic PCR and DNA sequencing

For confirming and sequencing *grgA* alleles in the chromosome and plasmid, total DNA was extracted from ~1,000 infected cells using the Quick-gDNA MiniPrep kit (Sigma Millipore) following manufacturer's instructions. The resulting DNA was used as template for PCR amplification using Taq DNA polymerase (Genscript). DNA fragments resolved with electrophoresis of 1.2% agarose gel purified using the Gel Extraction Kit (Qiagen) and subject to Sanger sequencing at Quintara Biosciences.

Quantification of chromosome and plasmid copy numbers

The chromosome copy number provides a quantitative measurement of the number of chlamydial cells, including RBs, EBs, and IBs, and is particularly useful for quantifying RB growth since RBs are non-infectious. To quantify chromosome copy numbers in cultures, infected cells were detached from 12-well plates using Cell Lifters (Corning). Cells and media were collected into Eppendorf tubes, centrifuged at 20,000 *g* at 4°C. The supernatant was carefully aspirated. One hundred microliters of alkaline lysis buffer (100 mM NaOH and 0.2 mM EDTA) was added into each tube to dissolve the cell pellets. Tubes were heated at 95°C for 15 min and then placed on ice. Three hundred fifty microliters of H_2O and 50 µL of 200 mM Tri-HCl (pH 7.2) were added into each tube and mixed. The neutralized extracts were used for qPCR analysis (1 µL/reaction) directly for samples collected up to 24 hpi or after a 100-fold dilution for samples collected thereafter. A pair of *ctl0631* primers (Table S5) was used for qPCR analysis to quantify chromosome copy numbers, while a pair of *pgp1* primers (Table S5) was used to quantify plasmid copy numbers. qPCR analysis was performed with biological triplicates and technical duplicates using QuantStudio five real-time PCR System and Power SYBR Green PCR Master Mix (ThermoFisher Bioscientific) (14, 34).

We took advantage of the pGrgA-DOPE plasmid to quantify the plasmid-to-chromosome ratio without preparing chlamydial chromosomal DNA free of host DNA contamination. Briefly, a pair of *grg*A primers and the aforementioned *pgp1* primers were simultaneously used to quantify pGrgA-DOPE prepared from *Escherichia coli*, while the *grgA* primers (Table S5) and the aforementioned *ctl0631* primers were simultaneously used to quantify chromosome of wild-type *C. trachomatis*. These analyses showed that the *grgA* primers and *pgp1* primers have the same amplification efficiencies for quantifying pGrgA-DOPE, while the *grgA* primers is 30% more efficient than the *ctl0631* primers in amplifying the chromosome. To determine plasmid-to-chromosome ratio in L2/cgad-peig, we ran qPCR analysis for *pgp1* and *ctl0631* simultaneously. We calculated plasmid-to-chromosome ratios by correcting the *ctl0631* amplification efficiency with *grgA* amplification efficiency.

C. trachomatis lipid metabolic labeling

Metabolic labeling of chlamydiae with the green-fluorescing lipid (N-[7-(4-nitrobenzo-2-oxa-1,3-diazole)]) aminocaproylsphingosine (C6-NBD-ceramide) (Invitrogen)

was performed as previously described with minor modifications (37, 38). We combined C6-NBD-ceramide with 0.034% defatted bovine serum albumin (dfBSA), which was prepared by twice washing BSA manufactured through heat shock with 100% ethanol. The complex contained 5 µM C6-NBD-ceramide and 5 µM dfBSA. HeLa cells infected with L2/cgad-peig were cultured in ATC-containing and ATC-free full medium (i.e., DMEM containing 10% fetal bovine serum and 1 µg/mL cycloheximide) for 17.5 and 27.5 h, respectively. Following the removal of the full medium, infected cells were incubated with the dfBSA/C6-NBD-ceramide complex at 4°C for 30 min, washed with PBS, and incubated in DMEM containing 0.34% dfBSA plus or minus 1 nM ATC for 6 h to "back-exchange" excess label from the plasma membrane. Fluorescence imaging was performed at 24 and 34 hpi for ATC+ and ATC− cultures, respectively.

Western blotting

Detection of MOMP and GrgA was performed as previously described (34). *Chlamydia*-infected cells in each well were harvested in 200 µL of 1× SDS-PAGE sample buffer, heated at 95°C for 5 min, and sonicated for 1 min (5 s on/5 s off) at 35% amplitude. Proteins were resolved in 10% SDS-PAGE gels and thereafter transferred onto polyvinylidene difluoride membranes. The membrane was probed with the monoclonal mouse anti-MOMP MC22 antibody (74), stripped, and reprobed with a polyclonal mouse anti-GrgA antibody (34).

Transmission electron microscopy

To visualize intracellular chlamydiae up to 36 hpi, L929 cell monolayers grown on six-well plates were infected as described above and cultured with medium supplemented with or without 1 nM ATC. For cultures up to 36 h, cells were removed from the plastic surface using trypsin, collected in PBS containing 10% fetal bovine serum, and centrifuged for 10 min at 500 *g*. Pelleted cells were resuspended in EM fixation buffer (2.5% glutaraldehyde, 4% paraformaldehyde, 0.1 M cacodylate buffer) at RT, allowed to incubate for 2 h, and stored at 4°C overnight. To visualize intracellular chlamydiae at 45 and 60 hpi, the above procedures resulted in lysis of infected cells and inclusions. To overcome this problem, cells grown on glass coverslips were infected with and fixed without trypsinization. To prepare samples for imaging, cells were first rinsed in 0.1 M cacodylate buffer, dehydrated in a graded series of ethanol, and then embedded in Eponate 812 resin at 68°C overnight. Ninety-nanometer thin sections were cut on a Leica UC6 microtome and picked up on a copper grid. Grids were stained with uranyl acetate followed by lead citrate. TIFF images were acquired on a Philips CM12 electron microscope at 80 kV using an AMT XR111 digital camera. EBs, RBs, and IBs were enumerated.

RNA isolation

Total host and chlamydial RNA were isolated from L2/cgad-peig-infected HeLa cells using TRI reagent (Millipore Sigma). DNA decontamination was achieved by two cycles of DNase I-XT (New England Biolabs) digestion. Complete removal of genomic DNA was confirmed by PCR analysis. RNA concentration was determined using Qubit RNA assay kits (ThermoFisher). Aliquots of the DNA-free RNA samples were stored at −80°C.

RNA sequencing and analyses

RNA-Seq was performed as described with minor modifications (14, 49). Briefly, total RNA integrity was determined using Fragment Analyzer (Agilent) prior to RNA-Seq library preparation. Illumina MRZE706 Ribo-Zero Gold Epidemiology rRNA Removal kit was used to remove mouse and chlamydial rRNAs. Oligo(dT) beads were used to remove mouse mRNA. RNA-Seq libraries were prepared using Illumina TruSeq stranded mRNA-Seq sample preparation protocol, subjected to quantification process, pooled for cBot amplification, and sequenced with Illumina Novoseq platform with 100 bp pair-end sequencing module. Short read sequences were first aligned to the CtL2 434/Bu

genome including the chromosome (GCF_000068585.1_ASM6858v1), the pL2 plasmid (AM886278), and four genes cloned into the plasmid (*his-grgA*, *bla*, *tetR* and the mKate gene) using STAR version 2.7.5a and then quantified for gene expression by HTSeq to obtain raw read counts per gene, and then converted to FPKM (Fragment Per Kilobase of gene length per Million reads of the library) (75–77). DESeq2, an R package commonly used for analysis of data from RNA-Seq studies and test for differential expression (78), was used to normalize data and find group-pairwise differential gene expression based on three criteria: $P < 0.05$, average FPKM >1, and fold change ≥1.

qRT-PCR analysis

qRT-PCR was performed using QuantStudio 5 real-time PCR System (ThermoFisher Bioscientific) and Luna Universal one-step qRT-PCR kit (New England BioLabs) as previously described (14, 34). Refer to Table S5 for information for qRT-PCR primers.

Statistical analysis

For the evaluation of progeny EBs, plasmid-to-chromosome ratios, qPCR results, qRT-PCR results, inclusion areas, and inclusion mKate intensities, *t*-tests were conducted using Microsoft Office Excel. Where applicable, *P*-values were adjusted for multiple comparisons by Benjamini-Hochberg procedure to control the false discovery rate.

ACKNOWLEDGMENTS

We thank Rajesh Patel (Rutgers – RWJMS EM Core Facility) for processing electron microscopy samples, Matthew Pan and Lingling Wang for determining the growth of eL2/cgad-peig, Dr. Derek Fisher (Southern Illinois University) for pDFTT3(aadA), Dr. Guangming Zhong (University of Texas Health Sciences Center San Antonio) for the polyclonal anti-GrgA antibody and monoclonal MC22 anti-MOMP, and Dr. Harlan D. Caldwell (National Institute of Allergy and Infectious Diseases) for the monoclonal L21-5 anti-MOMP antibody.

We also acknowledge Tara Kehair's participation in the analysis of electron microscopic images.

This work was supported by grants from the National Institutes of Health (grant numbers AI140167 and AI154305 to H.F. and GM142702 to V.W.L.).

RNA-Seq data were generated in the Genome Sequencing Facility, which is supported by UT Health San Antonio, NIH-NCI P30 CA054174 (Cancer Center at UT Health San Antonio) and NIH Shared Instrument grant S10OD030311 (S10 grant to NovaSeq 6000 System), and CPRIT Core Facility Award (RP220662).

X.W. is supported by National Natural Sciences Foundation of China (grant number 32370197)

AUTHOR AFFILIATIONS

[1]Department of Parasitology, Central South University Xiangya Medical School, Changsha, Hunan, China
[2]Department of Pharmacology, Robert Wood Johnson Medical School, Rutgers, The State University of New Jersey, Piscataway, New Jersey, USA
[3]Greehey Children's Cancer Research Institute, University of Texas Health San Antonio, San Antonio, Texas, USA
[4]Department of Molecular Medicine, University of Texas Health San Antonio, San Antonio, Texas, USA
[5]Department of Statistics, University of California Riverside, Riverside, California, USA

PRESENT ADDRESS

Wurihan Wurihan, Department of Microbiology, Yangzhou University School of Medicine, Yangzhou, Jiangsu, China

AUTHOR ORCIDs

Bin Lu http://orcid.org/0000-0002-3193-3941
Yuxuan Wang http://orcid.org/0000-0003-0771-1078
Andrew Cheng http://orcid.org/0000-0002-9155-6156
Joseph D. Fondell http://orcid.org/0000-0002-7046-9854
Danny Wan http://orcid.org/0000-0001-8262-8173
Xiang Wu http://orcid.org/0000-0001-8218-5288
Wei Vivian Li http://orcid.org/0000-0002-2087-2709
Huizhou Fan http://orcid.org/0000-0002-4903-926X

FUNDING

Funder	Grant(s)	Author(s)
HHS | National Institutes of Health (NIH)	AI140167, AI154305	Huizhou Fan
HHS | National Institutes of Health (NIH)	GM142702	Vivian Wei Li
HHS | National Institutes of Health (NIH)	CA054174, S10OD030311	Zhao Lai
Cancer Prevention and Research Institute of Texas (CPRIT)	RP220662	Zhao Lai
MOST | National Natural Science Foundation of China (NSFC)	32370197	Xiang Wu

DATA AVAILABILITY

RNA-Seq data have been deposited into the NCBI Gene Expression Omnibus under accession number GSE234589.

ADDITIONAL FILES

The following material is available online.

Supplemental Material

Figure S1 (mBio02036-23-s0001.pdf). Map of the shuttle plasmid pGrgA-DOPE.
Figure S2 (mBio02036-23-s0002.pdf). Optimization of the ATC-inducible expression system for DOPE of GrgA.
Figure S3 (mBio02036-23-s0003.pdf). ATC-induced GrgA expression from pGrgA-DOPE in L2/cg-peig does not affect chlamydial growth.
Figure S4 (mBio02036-23-s0004.pdf). Confirmation of upregulated euo and hrcA expression in response to GrgA deficiency during midcycle.
Table S1 (mBio02036-23-s0005.xlsx). All RNA-Seq data.
Table S2 (mBio02036-23-s0006.xlsx). Numerous late genes are insufficiently activated from midcycle to early developmental cycle points identified by RNA-Seq.
Table S3 (mBio02036-23-s0007.xlsx). Genes with decreased expression at early late development stage due to GrgA deficiency.
Table S4 (mBio02036-23-s0008.xlsx). Genes with increased expression at midcycle due to GrgA deficiency.
Table S5 (mBio02036-23-s0009.xlsx). Expression changes of Pgp4 target genes in GrgA-deficient chlamydiae.
Table S6 (mBio02036-23-s0010.xlsx). Primers used for this study.

REFERENCES

1. Abdelrahman YM, Belland RJ. 2005. The chlamydial developmental cycle. FEMS Microbiol Rev 29:949–959. https://doi.org/10.1016/j.femsre.2005.03.002
2. Hackstadt T, Baehr W, Ying Y. 1991. *Chlamydia trachomatis* developmentally regulated protein is homologous to eukaryotic histone H1. Proc Natl Acad Sci U S A 88:3937–3941. https://doi.org/10.1073/pnas.88.9.3937
3. Hackstadt T, Brickman TJ, Barry CE, Sager J. 1993. Diversity in the *Chlamydia trachomatis* histone homologue Hc2. Gene 132:137–141. https://doi.org/10.1016/0378-1119(93)90526-9
4. Lambden PR, Everson JS, Ward ME, Clarke IN. 1990. Sulfur-rich proteins of *Chlamydia trachomatis*: developmentally regulated transcription of polycistronic mRNA from tandem promoters. Gene 87:105–112. https://doi.org/10.1016/0378-1119(90)90500-q
5. Lee JK, Enciso GA, Boassa D, Chander CN, Lou TH, Pairawan SS, Guo MC, Wan FYM, Ellisman MH, Sütterlin C, Tan M. 2018. Replication-dependent size reduction precedes differentiation in *Chlamydia trachomatis*. Nat Commun 9:45. https://doi.org/10.1038/s41467-017-02432-0
6. Belland RJ, Zhong G, Crane DD, Hogan D, Sturdevant D, Sharma J, Beatty WL, Caldwell HD. 2003. Genomic transcriptional profiling of the developmental cycle of *Chlamydia trachomatis*. Proc Natl Acad Sci U S A 100:8478–8483. https://doi.org/10.1073/pnas.1331135100
7. Nicholson TL, Olinger L, Chong K, Schoolnik G, Stephens RS. 2003. Global stage-specific gene regulation during the developmental cycle of *Chlamydia trachomatis*. J Bacteriol 185:3179–3189. https://doi.org/10.1128/JB.185.10.3179-3189.2003
8. Darst SA. 2001. Bacterial RNA polymerase. Curr Opin Struct Biol 11:155–162. https://doi.org/10.1016/s0959-440x(00)00185-8
9. Stephens RS, Kalman S, Lammel C, Fan J, Marathe R, Aravind L, Mitchell W, Olinger L, Tatusov RL, Zhao Q, Koonin EV, Davis RW. 1998. Genome sequence of an obligate intracellular pathogen of humans: *Chlamydia trachomatis*. Science 282:754–759. https://doi.org/10.1126/science.282.5389.754
10. Thomson NR, Holden MTG, Carder C, Lennard N, Lockey SJ, Marsh P, Skipp P, O'Connor CD, Goodhead I, Norbertzcak H, Harris B, Ormond D, Rance R, Quail MA, Parkhill J, Stephens RS, Clarke IN. 2008. *Chlamydia trachomatis*: genome sequence analysis of lymphogranuloma venereum isolates. Genome Res 18:161–171. https://doi.org/10.1101/gr.7020108
11. Soules KR, LaBrie SD, May BH, Hefty PS. 2020. Sigma 54-regulated transcription is associated with membrane reorganization and type III secretion effectors during conversion to infectious forms of *Chlamydia trachomatis*. mBio 11:e01725-20. https://doi.org/10.1128/mBio.01725-20
12. Yu HHY, Tan M. 2003. Sigma28 RNA polymerase regulates hctB, a late developmental gene in *Chlamydia*. Mol Microbiol 50:577–584. https://doi.org/10.1046/j.1365-2958.2003.03708.x
13. Shen L, Feng X, Yuan Y, Luo X, Hatch TP, Hughes KT, Liu JS, Zhang YX. 2006. Selective promoter recognition by chlamydial sigma28 holoenzyme. J Bacteriol 188:7364–7377. https://doi.org/10.1128/JB.01014-06
14. Wurihan W, Zou Y, Weber AM, Weldon K, Huang Y, Bao X, Zhu C, Wu X, Wang Y, Lai Z, Fan H. 2021. Identification of a Grga-Euo-Hrca transcriptional regulatory network in *Chlamydia*. mSystems 6:e0073821. https://doi.org/10.1128/mSystems.00738-21
15. Desai M, Wurihan W, Di R, Fondell JD, Nickels BE, Bao X, Fan H. 2018. Role for GrgA in regulation of σ^{28}-dependent transcription in the obligate intracellular bacterial pathogen *Chlamydia trachomatis*. J Bacteriol 200:e00298-18. https://doi.org/10.1128/JB.00298-18
16. Bao X, Nickels BE, Fan H. 2012. *Chlamydia trachomatis* protein GrgA activates transcription by contacting the nonconserved region of σ^{66}. Proc Natl Acad Sci U S A 109:16870–16875. https://doi.org/10.1073/pnas.1207300109
17. Rosario CJ, Hanson BR, Tan M. 2014. The transcriptional repressor EUO regulates both subsets of *Chlamydia* late genes. Mol Microbiol 94:888–897. https://doi.org/10.1111/mmi.12804
18. Hanson BR, Tan M. 2015. Transcriptional regulation of the *Chlamydia* heat shock stress response in an intracellular infection. Mol Microbiol 97:1158–1167. https://doi.org/10.1111/mmi.13093
19. Lund PA. 2001. Microbial molecular chaperones. Adv Microb Physiol 44:93–140. https://doi.org/10.1016/s0065-2911(01)44012-4
20. Fisher DJ, Beare PA. 2023. Recent advances in genetic systems in obligate intracellular human-pathogenic bacteria. Front Cell Infect Microbiol 13:1202245. https://doi.org/10.3389/fcimb.2023.1202245
21. Wan W, Li D, Li D, Jiao J. 2023. Advances in genetic manipulation of *Chlamydia trachomatis*. Front Immunol 14:1209879. https://doi.org/10.3389/fimmu.2023.1209879
22. Zhong J, Karberg M, Lambowitz AM. 2003. Targeted and random bacterial gene disruption using a group II intron (targetron) vector containing a retrotransposition-activated selectable marker. Nucleic Acids Res 31:1656–1664. https://doi.org/10.1093/nar/gkg248
23. Kokes M, Dunn JD, Granek JA, Nguyen BD, Barker JR, Valdivia RH, Bastidas RJ. 2015. Integrating chemical mutagenesis and whole-genome sequencing as a platform for forward and reverse genetic analysis of *Chlamydia*. Cell Host Microbe 17:716–725. https://doi.org/10.1016/j.chom.2015.03.014
24. Johnson CM, Fisher DJ. 2013. Site-specific, insertional inactivation of incA in *Chlamydia trachomatis* using a group II Intron. PLoS One 8:e83989. https://doi.org/10.1371/journal.pone.0083989
25. Cossé MM, Barta ML, Fisher DJ, Oesterlin LK, Niragire B, Perrinet S, Millot GA, Hefty PS, Subtil A. 2018. The loss of expression of a single type 3 effector (CT622) strongly reduces *Chlamydia trachomatis* infectivity and growth. Front Cell Infect Microbiol 8:145. https://doi.org/10.3389/fcimb.2018.00145
26. Thompson CC, Griffiths C, Nicod SS, Lowden NM, Wigneshweraraj S, Fisher DJ, McClure MO. 2015. The Rsb Phosphoregulatory network controls availability of the primary sigma factor in *Chlamydia trachomatis* and influences the Kinetics of growth and development. PLoS Pathog 11:e1005125. https://doi.org/10.1371/journal.ppat.1005125
27. Sixt BS, Bastidas RJ, Finethy R, Baxter RM, Carpenter VK, Kroemer G, Coers J, Valdivia RH. 2017. The *Chlamydia trachomatis* inclusion membrane protein CpoS counteracts STING-mediated cellular surveillance and suicide programs. Cell Host Microbe 21:113–121. https://doi.org/10.1016/j.chom.2016.12.002
28. DeBoer AG, Lei L, Yang C, Martens CA, Anzick SL, Antonioli-Schmit S, Suchland RJ, McClarty G, Caldwell HD, Rockey DD. 2023. Targetron inactivation of *Chlamydia trachomatis* gseA results in a lipopolysaccharide 3-Deoxy-d-Manno-Oct-2-ulosonic acid-deficient strain that is cytotoxic for cells. Infect Immun 91:e0009623. https://doi.org/10.1128/iai.00096-23
29. Weber MM, Lam JL, Dooley CA, Noriea NF, Hansen BT, Hoyt FH, Carmody AB, Sturdevant GL, Hackstadt T. 2017. Absence of specific *Chlamydia trachomatis* inclusion membrane proteins triggers premature inclusion membrane lysis and host cell death. Cell Rep 19:1406–1417. https://doi.org/10.1016/j.celrep.2017.04.058
30. Shaw JH, Key CE, Snider TA, Sah P, Shaw EI, Fisher DJ, Lutter EI. 2018. Genetic inactivation of *Chlamydia trachomatis* inclusion membrane protein CT228 alters MYPT1 recruitment, extrusion production, and longevity of infection. Front Cell Infect Microbiol 8:415. https://doi.org/10.3389/fcimb.2018.00415
31. Zhong G. 2017. Chlamydial plasmid-dependent pathogenicity. Trends Microbiol. 25:141–152. https://doi.org/10.1016/j.tim.2016.09.006
32. Song L, Carlson JH, Whitmire WM, Kari L, Virtaneva K, Sturdevant DE, Watkins H, Zhou B, Sturdevant GL, Porcella SF, McClarty G, Caldwell HD. 2013. *Chlamydia trachomatis* plasmid-encoded Pgp4 is a transcriptional regulator of virulence-associated genes. Infect Immun 81:636–644. https://doi.org/10.1128/IAI.01305-12
33. Turman BJ, Darville T, O'Connell CM. 2023. Plasmid-mediated virulence in *Chlamydia*. Front Cell Infect Microbiol 13:1251135. https://doi.org/10.3389/fcimb.2023.1251135
34. Wurihan W, Weber AM, Gong Z, Lou Z, Sun S, Zhou J, Fan H. 2021. Grga overexpression inhibits *Chlamydia trachomatis* growth through Sigma66- and Sigma28-dependent mechanisms. Microbial Pathogenesis 156:104917. https://doi.org/10.1016/j.micpath.2021.104917
35. Wang Y, Kahane S, Cutcliffe LT, Skilton RJ, Lambden PR, Clarke IN, Valdivia RH. 2011. Development of a transformation system for *Chlamydia trachomatis*: restoration of glycogen biosynthesis by acquisition of a plasmid shuttle vector. PLoS Pathog 7:e1002258. https://doi.org/10.1371/journal.ppat.1002258

36. Wickstrum J, Sammons LR, Restivo KN, Hefty PS. 2013. Conditional gene expression in *Chlamydia trachomatis* using the TET system. PLoS One 8:e76743. https://doi.org/10.1371/journal.pone.0076743
37. Rockey DD, Fischer ER, Hackstadt T. 1996. Temporal analysis of the developing *Chlamydia psittaci* inclusion by use of fluorescence and electron microscopy. Infect Immun 64:4269–4278. https://doi.org/10.1128/iai.64.10.4269-4278.1996
38. Hackstadt T, Scidmore MA, Rockey DD. 1995. Lipid metabolism in *Chlamydia trachomatis*-infected cells: directed trafficking of golgi-derived sphingolipids to the chlamydial inclusion. Proc Natl Acad Sci U S A 92:4877–4881. https://doi.org/10.1073/pnas.92.11.4877
39. Pickett MA, Everson JS, Pead PJ, Clarke IN. 2005. The plasmids of *Chlamydia trachomatis* and *Chlamydophila pneumoniae* (N16): accurate determination of copy number and the paradoxical effect of plasmid-curing agents. Microbiology (Reading) 151:893–903. https://doi.org/10.1099/mic.0.27625-0
40. Swoboda AR, Wood NA, Saery EA, Fisher DJ, Ouellette SP. 2023. The periplasmic tail-specific protease, Tsp, is essential for secondary differentiation in *Chlamydia trachomatis*. J Bacteriol 205:e0009923. https://doi.org/10.1128/jb.00099-23
41. Chen YS, Bastidas RJ, Saka HA, Carpenter VK, Richards KL, Plano GV, Valdivia RH. 2014. The *Chlamydia trachomatis* type III secretion chaperone Slc1 engages multiple early effectors, including TepP, a tyrosine-phosphorylated protein required for the recruitment of Crki-II to nascent inclusions and innate immune signaling. PLoS Pathog 10:e1003954. https://doi.org/10.1371/journal.ppat.1003954
42. Lutter EI, Barger AC, Nair V, Hackstadt T. 2013. *Chlamydia trachomatis* inclusion membrane protein CT228 recruits elements of the myosin phosphatase pathway to regulate release mechanisms. Cell Rep 3:1921–1931. https://doi.org/10.1016/j.celrep.2013.04.027
43. Clifton DR, Fields KA, Grieshaber SS, Dooley CA, Fischer ER, Mead DJ, Carabeo RA, Hackstadt T. 2004. A chlamydial type III translocated protein is tyrosine-phosphorylated at the site of entry and associated with recruitment of actin. Proc Natl Acad Sci U S A 101:10166–10171. https://doi.org/10.1073/pnas.0402829101
44. Lane BJ, Mutchler C, Al Khodor S, Grieshaber SS, Carabeo RA. 2008. Chlamydial entry involves TARP binding of guanine nucleotide exchange factors. PLoS Pathog 4:e1000014. https://doi.org/10.1371/journal.ppat.1000014
45. Elwell C, Mirrashidi K, Engel J. 2016. Chlamydia cell biology and pathogenesis. Nat Rev Microbiol 14:385–400. https://doi.org/10.1038/nrmicro.2016.30
46. Hatch ND, Ouellette SP. 2023. Identification of the alternative sigma factor regulons of *Chlamydia trachomatis* using multiplexed CRISPR interference. mSphere 8:e0039123. https://doi.org/10.1128/msphere.00391-23
47. Pokorzynski ND, Alla MR, Carabeo RA. 2022. Host cell amplification of nutritional stress contributes to persistence in *Chlamydia trachomatis*. mBio 13:e0271922. https://doi.org/10.1128/mbio.02719-22
48. Somboonna N, Ziklo N, Ferrin TE, Hyuk Suh J, Dean D. 2019. Clinical persistence of *Chlamydia trachomatis* sexually transmitted strains involves novel mutations in the functional AββA tetramer of the tryptophan synthase operon. mBio 10:e01464-19. https://doi.org/10.1128/mBio.01464-19
49. Huang Y, Wurihan W, Lu B, Zou Y, Wang Y, Weldon K, Fondell JD, Lai Z, Wu X, Fan H. 2021. Robust heat shock response in *Chlamydia* lacking a typical heat shock Sigma factor. Front Microbiol 12:812448. https://doi.org/10.3389/fmicb.2021.812448
50. Mueller KE, Wolf K, Fields KA. 2016. Gene deletion by fluorescence-reported allelic exchange mutagenesis in *Chlamydia trachomatis*. mBio 7:e01817–15. https://doi.org/10.1128/mBio.01817-15
51. Ouellette SP. 2018. Feasibility of a conditional knockout system for *Chlamydia* based on CRISPR interference. Front Cell Infect Microbiol 8:59. https://doi.org/10.3389/fcimb.2018.00059
52. Wang Y, LaBrie SD, Carrell SJ, Suchland RJ, Dimond ZE, Kwong F, Rockey DD, Hefty PS, Hybiske K. 2019. Development of transposon mutagenesis for *Chlamydia muridarum*. J Bacteriol 201:e00366-19. https://doi.org/10.1128/JB.00366-19
53. Cortina ME, Bishop RC, DeVasure BA, Coppens I, Derré I. 2022. The inclusion membrane protein Incs is critical for initiation of the *Chlamydia* intracellular developmental cycle. PLoS Pathog 18:e1010818. https://doi.org/10.1371/journal.ppat.1010818
54. Garvin L, Vande Voorde R, Dickinson M, Carrell S, Hybiske K, Rockey D. 2021. A broad-spectrum cloning vector that exists as both an integrated element and a free plasmid in *Chlamydia trachomatis*. PLoS One 16:e0261088. https://doi.org/10.1371/journal.pone.0261088
55. Ouellette SP, Blay EA, Hatch ND, Fisher-Marvin LA. 2021. CRISPR interference to Inducibly repress gene expression in *Chlamydia trachomatis*. Infect Immun 89:e0010821. https://doi.org/10.1128/IAI.00108-21
56. Wang L, Zhu C, Zhang T, Tian Q, Zhang N, Morrison S, Morrison R, Xue M, Zhong G. 2018. Nonpathogenic colonization with *Chlamydia* in the gastrointestinal tract as oral vaccination for inducing transmucosal protection. Infect Immun 86:e00630-17. https://doi.org/10.1128/IAI.00630-17
57. Nobles CL. 2021. iGUIDE method for CRISPR off-target detection. Methods Mol Biol 2189:71–80. https://doi.org/10.1007/978-1-0716-0822-7_6
58. Skilton RJ, Wang Y, O'Neill C, Filardo S, Marsh P, Bénard A, Thomson NR, Ramsey KH, Clarke IN. 2018. The *Chlamydia muridarum* plasmid revisited: new insights into growth kinetics. Wellcome Open Res 3:25. https://doi.org/10.12688/wellcomeopenres.13905.1
59. Zhang Q, Rosario CJ, Sheehan LM, Rizvi SM, Brothwell JA, He C, Tan M. 2020. The repressor function of the *Chlamydia* late regulator EUO is enhanced by the plasmid-encoded protein Pgp4. J Bacteriol 202:e00793-19. https://doi.org/10.1128/JB.00793-19
60. Chiarelli TJ, Grieshaber NA, Omsland A, Remien CH, Grieshaber SS. 2020. Single-inclusion kinetics of *Chlamydia trachomatis* development. mSystems 5:e00689-20. https://doi.org/10.1128/mSystems.00689-20
61. Kari L, Whitmire WM, Olivares-Zavaleta N, Goheen MM, Taylor LD, Carlson JH, Sturdevant GL, Lu C, Bakios LE, Randall LB, Parnell MJ, Zhong G, Caldwell HD. 2011. A live-attenuated chlamydial vaccine protects against trachoma in nonhuman primates. J Exp Med 208:2217–2223. https://doi.org/10.1084/jem.20111266
62. O'Connell CM, Ingalls RR, Andrews CW, Scurlock AM, Darville T. 2007. Plasmid-deficient *Chlamydia muridarum* fail to induce immune pathology and protect against oviduct disease. J Immunol 179:4027–4034. https://doi.org/10.4049/jimmunol.179.6.4027
63. Sigar IM, Schripsema JH, Wang Y, Clarke IN, Cutcliffe LT, Seth-Smith HMB, Thomson NR, Bjartling C, Unemo M, Persson K, Ramsey KH. 2014. Plasmid deficiency in urogenital isolates of *Chlamydia trachomatis* reduces infectivity and virulence in a mouse model. Pathog Dis 70:61–69. https://doi.org/10.1111/2049-632X.12086
64. Feklístov A, Sharon BD, Darst SA, Gross CA. 2014. Bacterial sigma factors: a historical, structural, and genomic perspective. Annu Rev Microbiol 68:357–376. https://doi.org/10.1146/annurev-micro-092412-155737
65. Mooney RA, Darst SA, Landick R. 2005. Sigma and RNA polymerase: an on-again, off-again relationship? Mol Cell 20:335–345. https://doi.org/10.1016/j.molcel.2005.10.015
66. Yu HHY, Kibler D, Tan M. 2006. *In silico* prediction and functional validation of sigma28-regulated genes in *Chlamydia* and *Escherichia coli*. J Bacteriol 188:8206–8212. https://doi.org/10.1128/JB.01082-06
67. Gerlach P, Søgaard-Andersen L, Pedersen H, Martinussen J, Valentin-Hansen P, Bremer E. 1991. The cyclic AMP (cAMP)-cAMP receptor protein complex functions both as an activator and as a corepressor at the tsx-P2 promoter of *Escherichia coli* K-12. J Bacteriol 173:5419–5430. https://doi.org/10.1128/jb.173.17.5419-5430.1991
68. Olliver A, Saggioro C, Herrick J, Sclavi B. 2010. DnaA-ATP acts as a molecular switch to control levels of ribonucleotide reductase expression in *Escherichia coli*. Mol Microbiol 76:1555–1571. https://doi.org/10.1111/j.1365-2958.2010.07185.x
69. van Kessel JC, Ulrich LE, Zhulin IB, Bassler BL. 2013. Analysis of activator and repressor functions reveals the requirements for transcriptional control by Luxr, the master regulator of quorum sensing in vibrio harveyi. mBio 4:e00378-13. https://doi.org/10.1128/mBio.00378-13
70. Troxell B, Hassan HM. 2013. Transcriptional regulation by ferric uptake regulator (fur) in pathogenic bacteria. Front Cell Infect Microbiol 3:59. https://doi.org/10.3389/fcimb.2013.00059
71. Lowden NM, Yeruva L, Johnson CM, Bowlin AK, Fisher DJ. 2015. Use of aminoglycoside 3′ adenyltransferase as a selection marker for *Chlamydia*

trachomatis intron-mutagenesis and *in vivo* intron stability. BMC Res Notes 8:570. https://doi.org/10.1186/s13104-015-1542-9
72. Caldwell HD, Kromhout J, Schachter J. 1981. Purification and partial characterization of the major outer membrane protein of *Chlamydia trachomatis*. Infect Immun 31:1161–1176. https://doi.org/10.1128/iai.31.3.1161-1176.1981
73. Zhang YX, Stewart S, Joseph T, Taylor HR, Caldwell HD. 1987. Protective monoclonal antibodies recognize epitopes located on the major outer membrane protein of *Chlamydia trachomatis*. J Immunol 138:575–581.
74. Zhong G, Fan P, Ji H, Dong F, Huang Y. 2001. Identification of a chlamydial protease-like activity factor responsible for the degradation of host transcription factors. J Exp Med 193:935–942. https://doi.org/10.1084/jem.193.8.935
75. Anders S, Pyl PT, Huber W. 2015. Htseq--a python framework to work with high-throughput sequencing data. Bioinformatics 31:166–169. https://doi.org/10.1093/bioinformatics/btu638
76. Anders S, Huber W. 2010. Differential expression analysis for sequence count data. Genome Biol. 11:R106–R106. https://doi.org/10.1186/gb-2010-11-10-r106
77. Trapnell C, Roberts A, Goff L, Pertea G, Kim D, Kelley DR, Pimentel H, Salzberg SL, Rinn JL, Pachter L. 2012. Differential gene and transcript expression analysis of RNA-seq experiments with tophat and cufflinks. Nat Protoc 7:562–578. https://doi.org/10.1038/nprot.2012.016
78. Love MI, Huber W, Anders S. 2014. Moderated estimation of fold change and dispersion for RNA-seq data with Deseq2. Genome Biol 15:550. https://doi.org/10.1186/s13059-014-0550-8